

Synthetic fluorescent probes for copper in biological systems

Literature seminar
2020/10/01
M2 Natsuki Konoue

➤ **Introduction**

➤ **Short summary**

➤ **Overview of advances in the development of Cu fluorescent indicators**

➤ **Summary**

Cu is an essential element for life

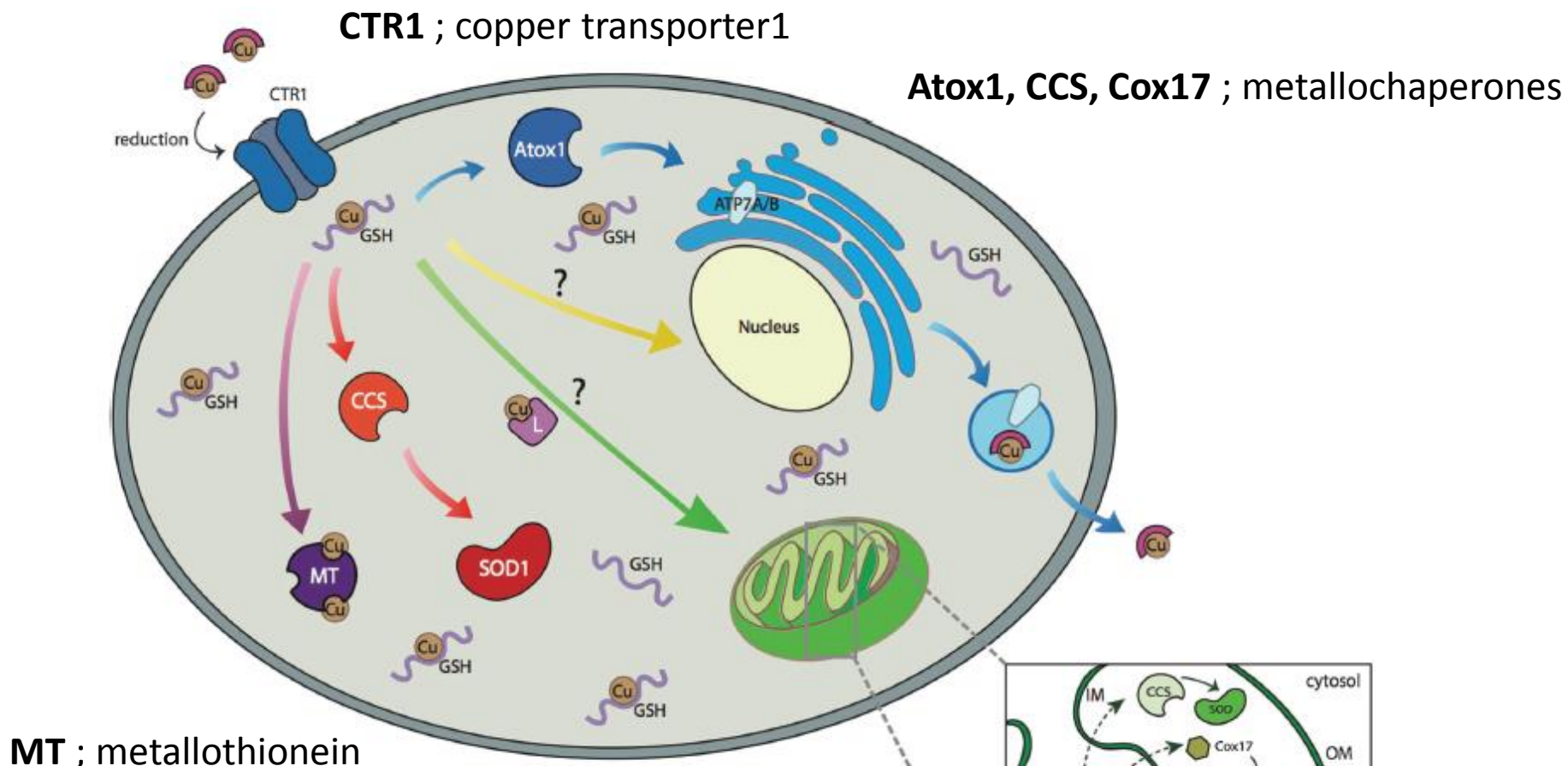
Cu serves as an essential cofactor for numerous redox enzymes that react with dioxygen and its reduced derivatives like superoxide

These enzymes are involved in critical processes

e.g.

- **Respiration**(cytochrome c oxidase)
- **Electron transfer/substrate oxidation**
- **Iron uptake**(celuroplasmin)
- **Pigmentation**(tyrosinase)
- **Antioxidant defence**(Cu/Zn superoxide dismutase)
- **Neurotransmitter synthesis and metabolism**
(dopamine β -hydrorase, peptidylglycine α -amidating monooxygenase)
- **Epigenetic modification**(lysyl oxidase like 2)
- **Handling of dietary amine**(copper amine oxidase)

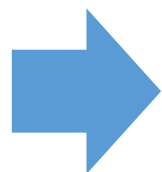
Overview of biological copper homeostasis ⁴



Cu trafficking is driven by affinity gradients from relatively weak ligand (CTR1, GSH) to tighter binding target protein (SOD1) *via* metallochaperones.

- **Genetic disorder** (Menkes and Wilson's disease)
- **Nurodegenerative disease** (Alzheimer's, Parkinson's, prion, and Huntigton's disease)
- **Familial amyotrophic lateral sclerosis; 家族性筋萎縮性側索硬化症**
- **Metabolic disorder**(obesity and diabetes)
- **Cancer**

Chem. Soc. Rev. **2015**, *44*, 4400–4414.



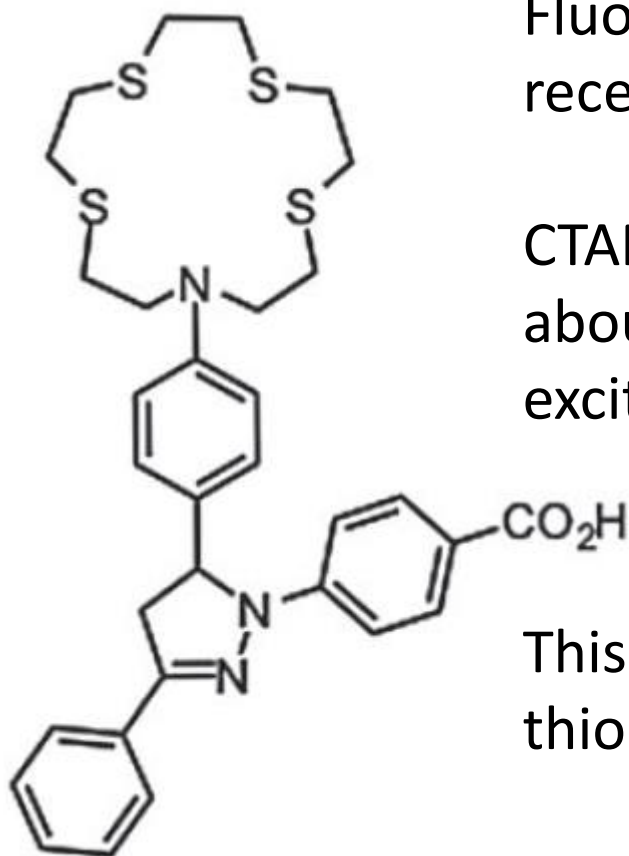
Understanding copper biology is important

- Copper redox activity is essential to maintaining normal physiological responses
- Copper misregulation is associated with various disease and disorder
- Copper homeostasis is tightly regulated by cells and tissues
- In addition to tightly bound pool of copper, reversibly and relatively loosely bound (“labile”) pool of copper in cells
- Sensing labile copper pools and understanding their functions using fluorescent indicators are important

Pyrazoline-based copper probes

7

CTAP-1 ; The first small-molecule fluorescent sensor for Cu(I)



Fluorophore : 1,3-diarylpyrazoline
receptor : tetrathiazacrown ether(NS4)

CTAP-1 features high selectivity for Cu(I) with about 5-fold turn-on response upon UV excitation at 365 nm

This work demonstrated the usefulness of thioether-rich motifs in copper sensor design.

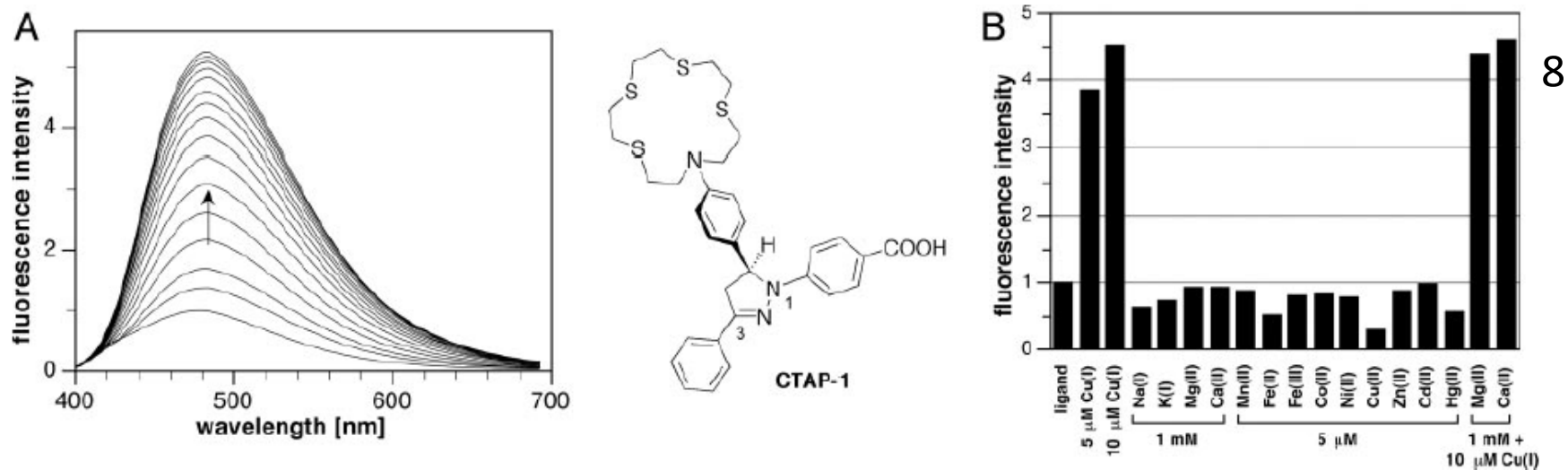
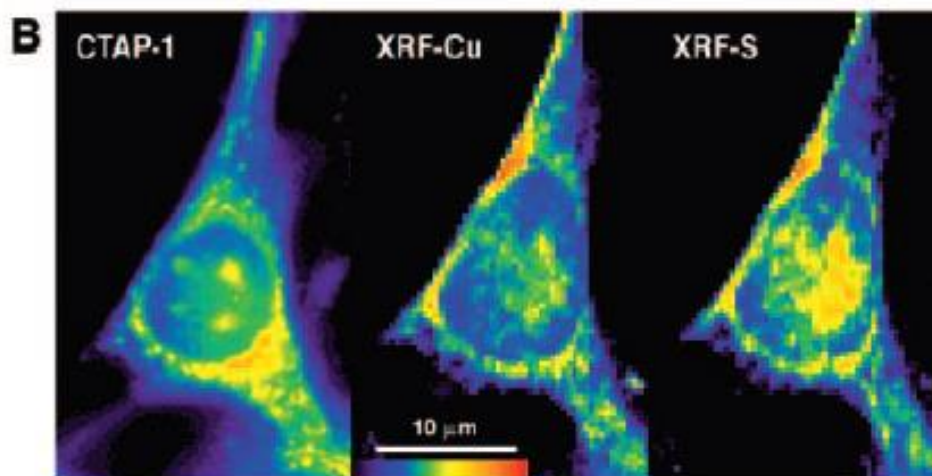
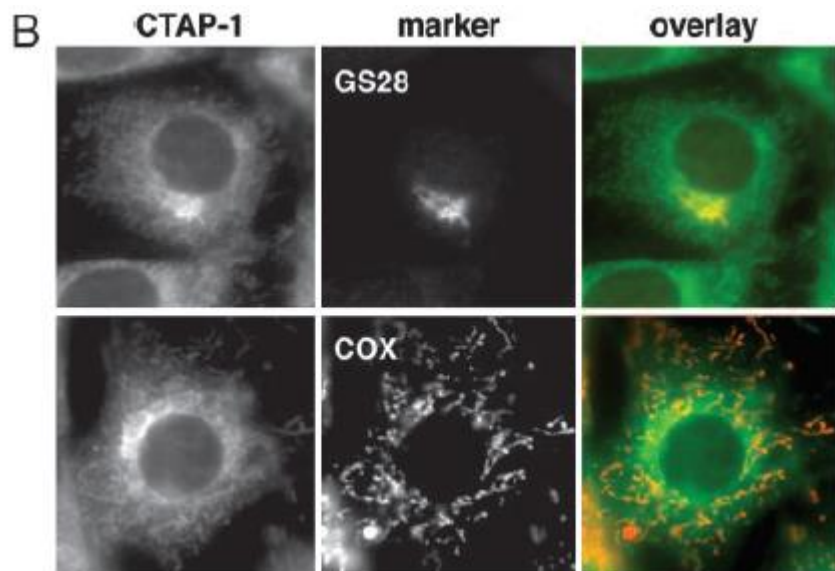
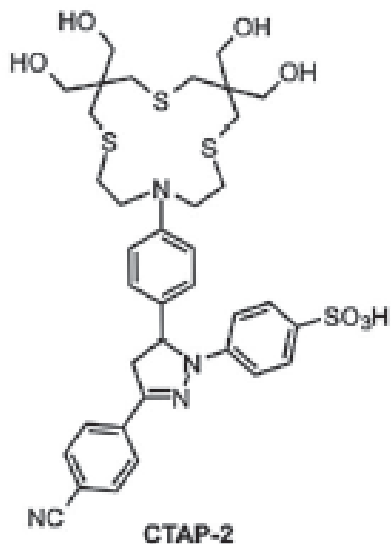


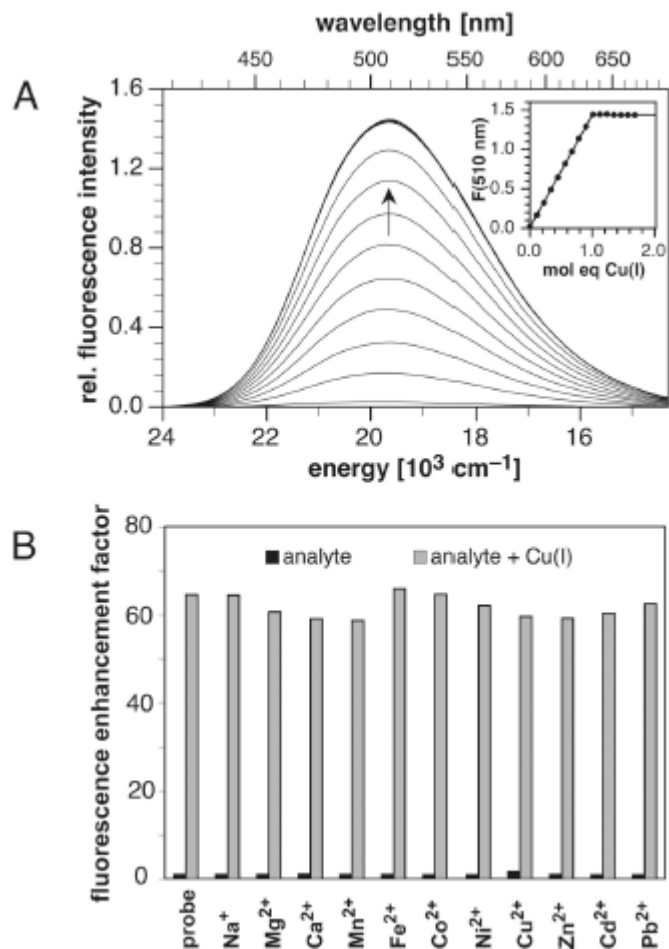
Fig. 1. Metal-dependent fluorescence response of CTAP-1. (A) (Left) Fluorescence emission spectra (λ_{ex} 365 nm) of CTAP-1 (5 μ M in 10 mM Pipes, pH 7.20, 25°C) as a function of added Cu(I) [0.1 molar eq aliquots of 5 mM Cu(CH₃CN)₄PF₆ in CH₃CN]. (Right) Structure of CTAP-1. (B) Emission response of CTAP-1 at 480 nm (λ_{ex} 365 nm) as a function of various added metal cations (5 μ M ligand/10 mM Pipes, pH 7.20).



(B) Immunofluorescence colocalization of the CTAP-1 staining pattern (Left) with two cellular marker antibodies (Center). (Upper) Anti-GS28 to visualize the Golgi apparatus. (Lower) Anti-OxPhos Complex V to visualize mitochondria (for details, see *Experimental Methods*). (Right) False coloroverlay (CTAP-1, green; antibody, red; areas of colocalization appear in orangeyellow).



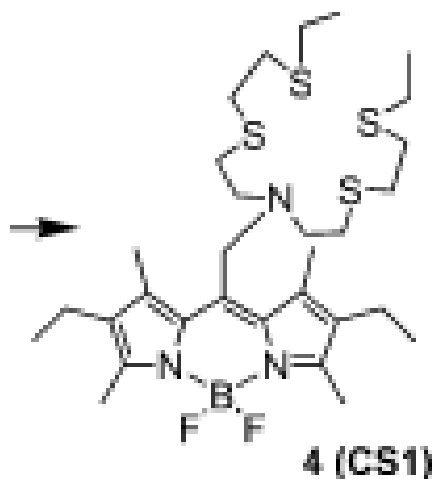
- Four hydroxymethyl groups were introduced to the tiazacrown receptor and a sulfonate moiety to the fluorophore
- This sensor could be dissolved directly in water instead of requiring dilution from an organic co-solvent.
- Not forming nano-scale colloidal aggregates that commonly occur with fluorescent dyes.



BODIPY-based copper sensors

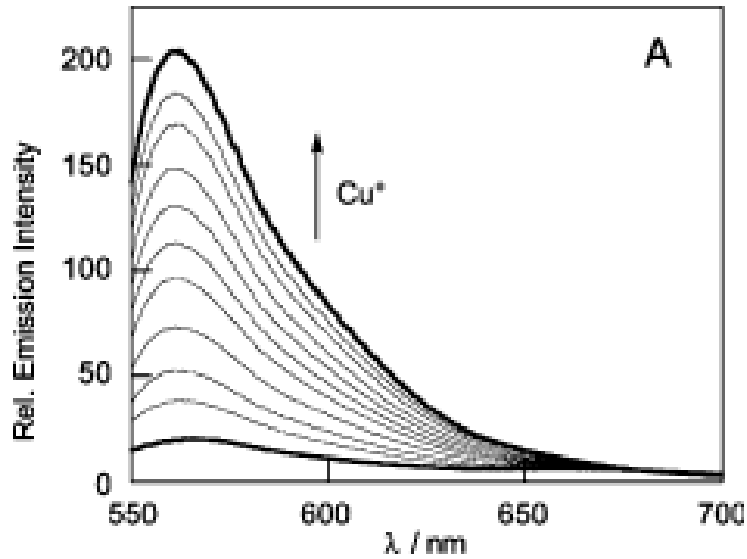
Coppersensor 1 (CS1) : the first example of a visible excitation/emission probe for Cu(I)

CS1 consists of a boron dipyrromethene (BODIPY)-based fluorophore coupled to the acyclic form of the NS₄ receptor; NS₄'



10-fold turn-on response and high selectivity for copper with visible excitation at 540 nm and emission at 561 nm

Proc. Natl. Acad. Sci. U. S. A., **2011**, *108*, 5980–5985.



Spectra shown are for buffered $[Cu^+]$ of 0, 0.2, 0.4, 0.6, 0.8, 1.0, 1.2, 1.4, 1.6, 1.8, and 2.0 μM

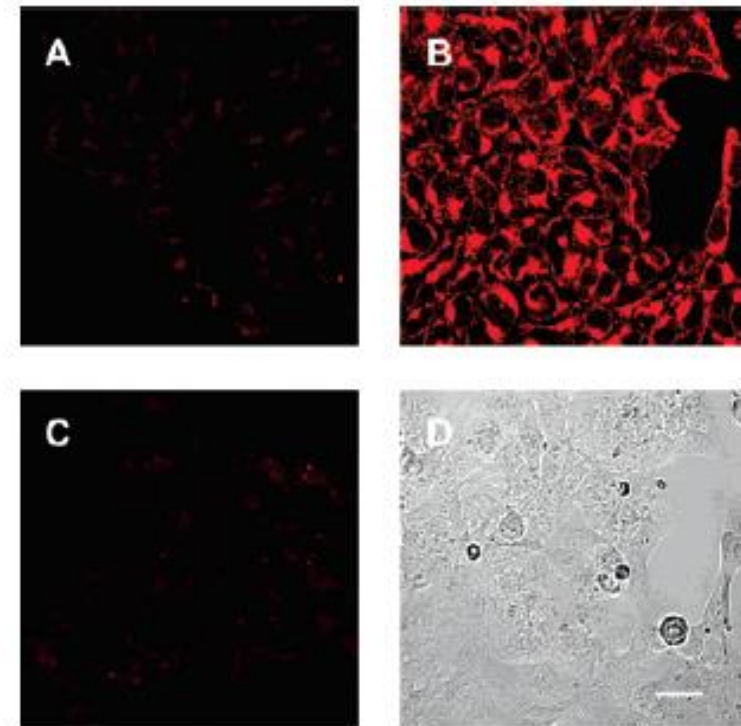
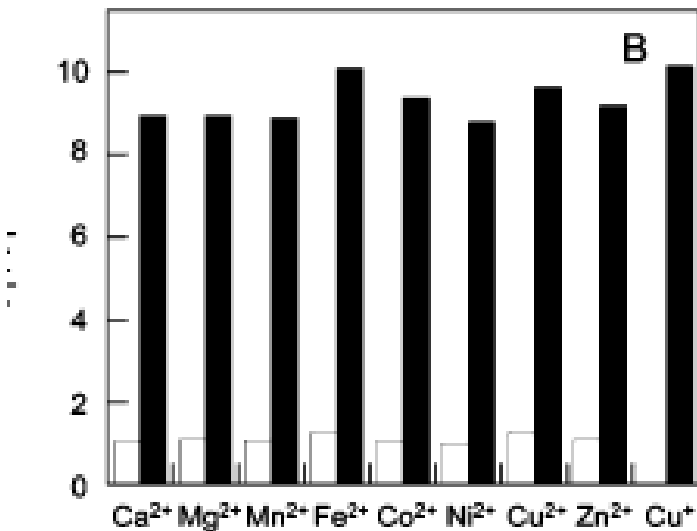


Figure 2. Confocal fluorescence images of live HEK 293 cells. (A) Cells incubated with 5 μM CS1 for 5 min at 25 $^{\circ}C$. (B) Cells supplemented with 100 μM $CuCl_2$ in the growth media for 7 h at 37 $^{\circ}C$ and stained with 5 μM CS1 for 5 min at 25 $^{\circ}C$. (C) $CuCl_2$ -supplemented cells pretreated with 500 μM of the competing Cu^+ chelator, 3,6,12,15-tetrathia-9-monoazaheptadecane, for 5 min at 25 $^{\circ}C$ before staining with 5 μM CS1 for 5 min at 25 $^{\circ}C$. (D) Brightfield image of live HEK 293 cells shown in panel B, confirming their viability. Scale bar = 25 μm .



White bars represent the addition of an excess of the appropriate metal ion (2 mM for Ca^{2+} , Mg^{2+} , and Zn^{2+} , 50 μM for all other cations) to a 2 μM solution of CS1. Black bars represent the subsequent addition of 10 μM Cu^+ to the solution.

CS1 fluorescence did not increase with increasing concentrations of CuCl_2 or $\text{Cu}^{\text{II}}(\text{gtsm})$ in some cells. 12

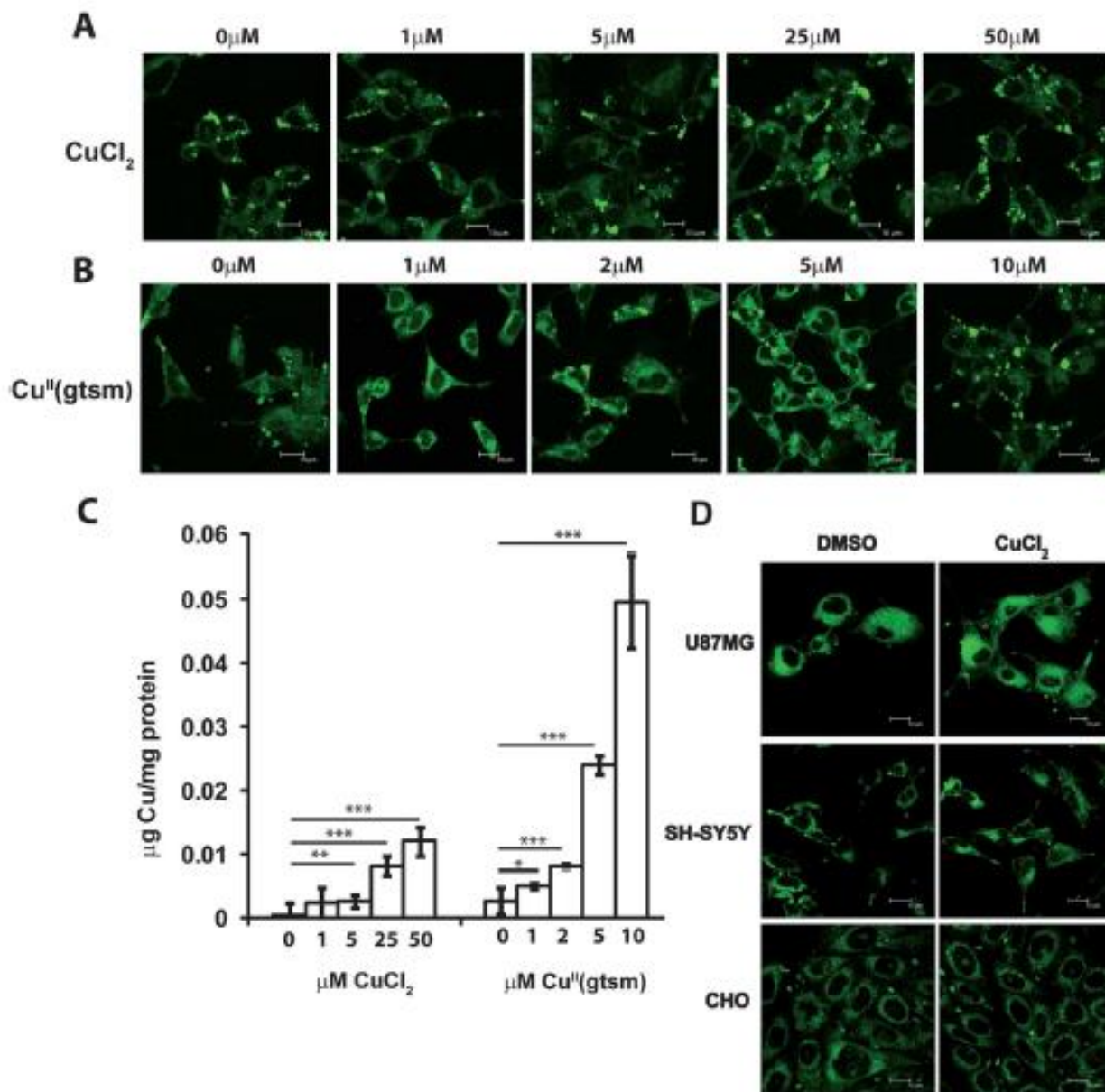
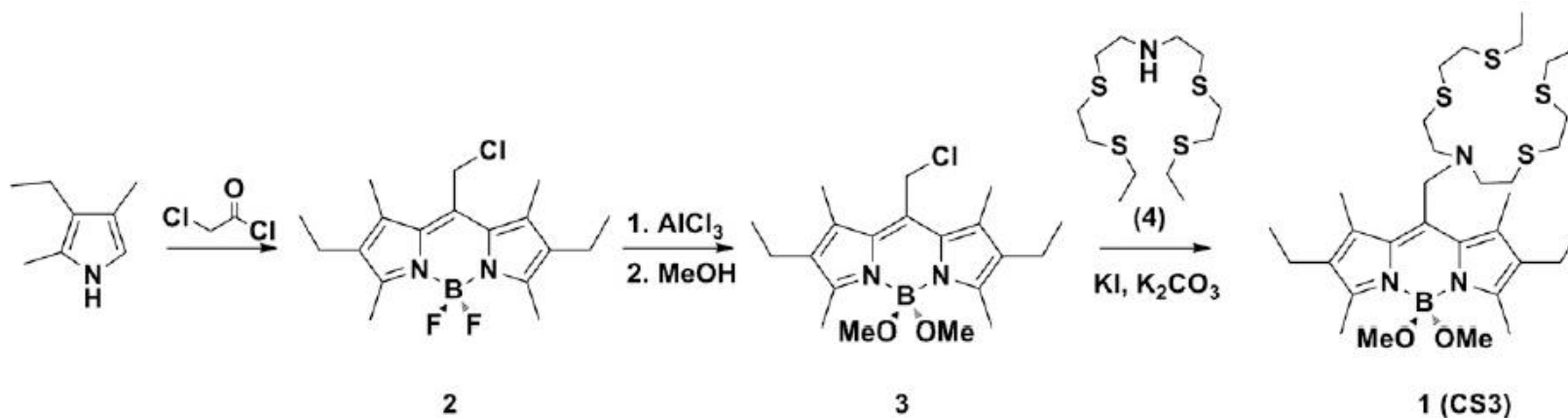


Fig. 3 CS1 fluorescence did not increase with increasing concentrations of CuCl_2 or $\text{Cu}^{\text{II}}(\text{gtsm})$ in M17 cells. Cells were treated with increasing concentrations of CuCl_2 (A), or $\text{Cu}^{\text{II}}(\text{gtsm})$ (B) for 30 min and CS1 (5 mM) was added for 5 min. Cells were fixed with 4% PFA and examined by confocal microscopy. No increase in fluorescence was observed in cultures treated with CuCl_2 or $\text{Cu}^{\text{II}}(\text{gtsm})$ at any concentration. Parallel measurement of cellular Cu levels by AAS showed a dose-dependent increase in Cu in CuCl_2 and $\text{Cu}^{\text{II}}(\text{gtsm})$ -treated cells (C). * $p < 0.05$, ** $p < 0.01$, *** $p < 0.001$ compared to vehicle control. (D) CS1 fluorescence was not enhanced in U87MG glial cells, SH-SY5Y neuronal-like cells or CHO epithelial cells supplemented with CuCl_2 . Cells were treated with CuCl_2 (100 mM) for 6 h. CS1 (5 mM) was added for the last 5 min of treatment. Cells were fixed with 4% PFA and examined for CS1 fluorescence by confocal microscopy.

Coppersensor 3(CS3) :

13

Boron centre were replaced by more electron-rich methoxy groups



This substitution improves water solubility and decreases the driving force for donor PET quenching of the fluorophore by increasing its electron density

CS3 exhibits improved turn-on response(75-fold for CS3 over 10-fold for CS1)

Higher quantum yield for the Cu(I) bound sensor ($\Phi=0.40$ for CS3, $\Phi=0.13$ for CS1)

Increasing binding affinity toward Cu(I) ($K_d=9 \times 10^{-14}$ M for CS3, $K_d=4 \times 10^{-12}$ M for CS1)

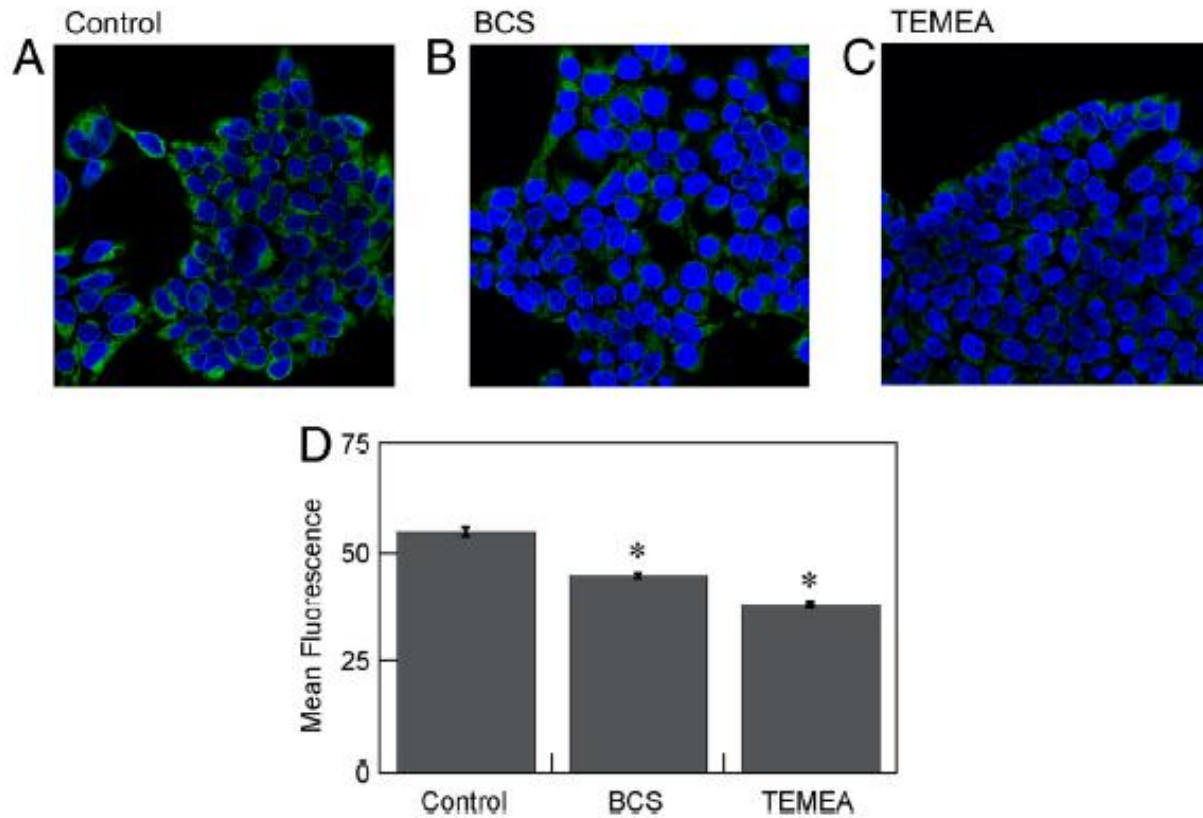


Fig. 3. Molecular imaging of endogenous basal Cu in HEK 293T cells with CS3. (A) Control HEK 293T cells, (B) HEK 293T cells supplemented with 200 μM BCS in the growth medium for 20 h at 37 $^{\circ}\text{C}$, and (C) HEK 293T cells treated with 100 μM TEMEA for 10 min. A, B, and C were stained with 2 μM CS3, 5 μM Hoechst 33342, and DMSO vehicle for TEMEA for 10 min at 37 $^{\circ}\text{C}$ in DMEM. (D) Graph showing the quantification of mean fluorescence intensity of each condition normalized to the control condition ($n = 5$ fields of cells per condition). Error bars represent the SEM. Asterisk (*) indicates $P < 0.01$ compared to control cells.

TEMEA ;
Copper chelator
tris((ethylthio)ethylam ine)

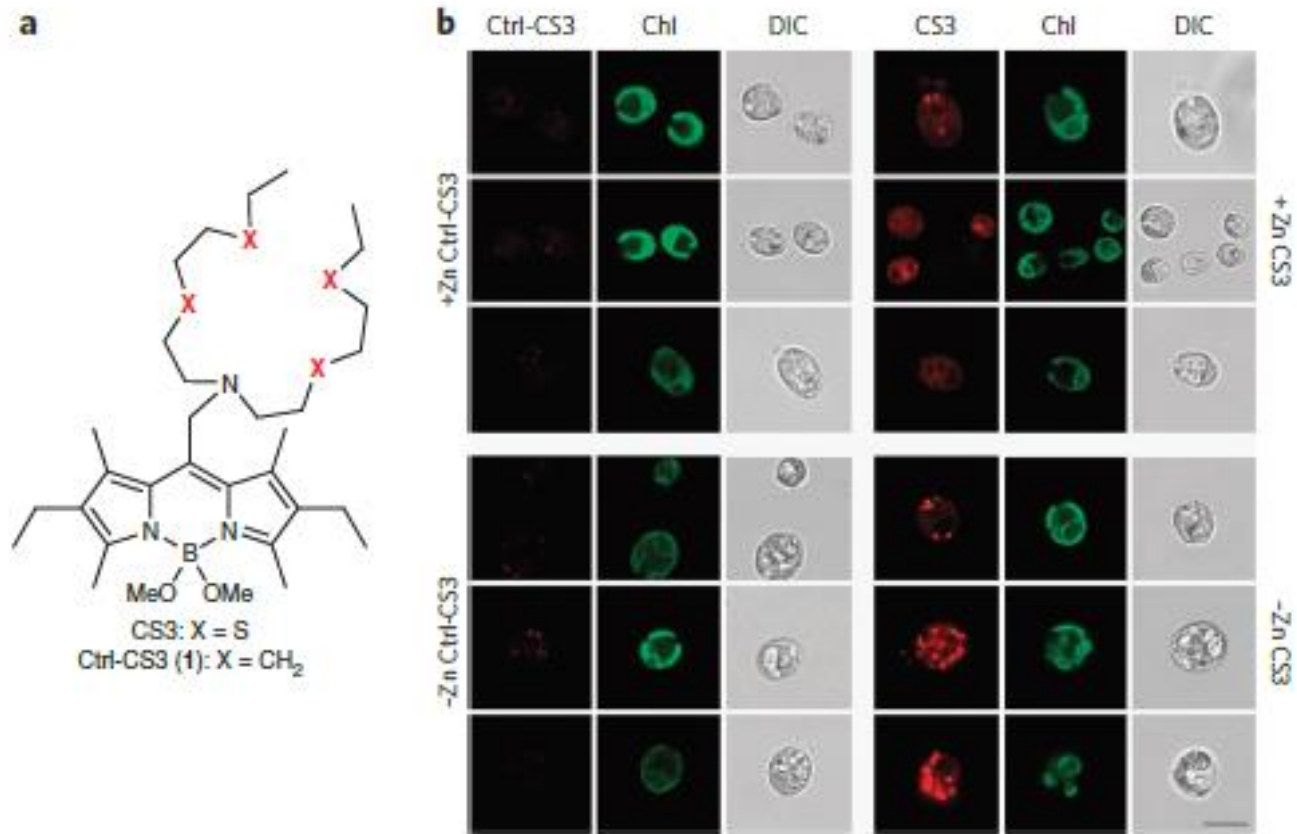
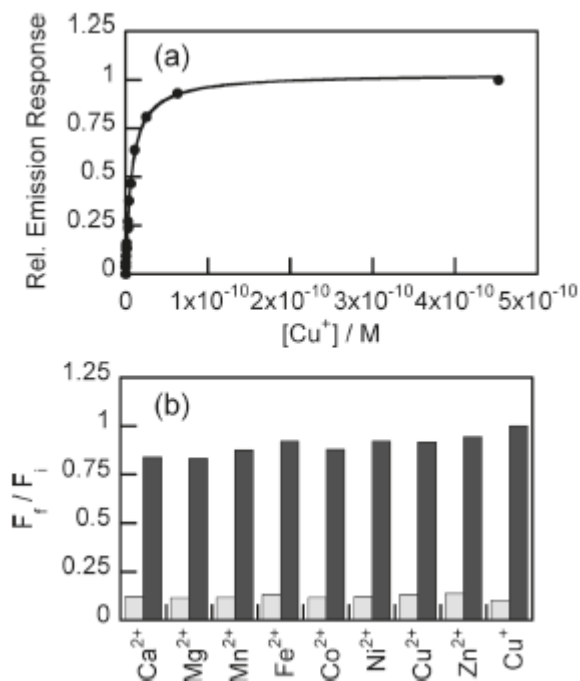
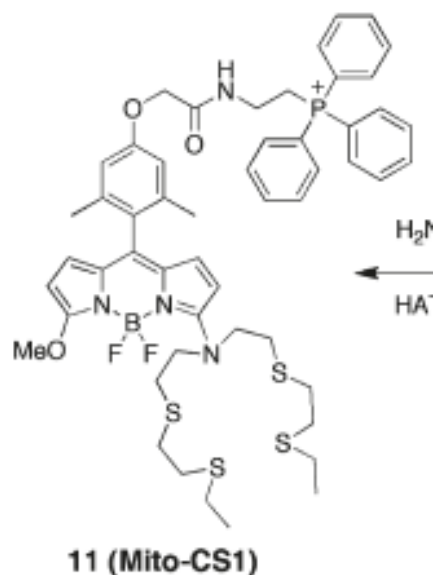


Figure 3 | Cu⁺-sensitive CS3 staining suggests Cu accumulation in intracellular compartments. (a) Chemical structure of the Cu⁺-binding fluorescent dye CS3 and the non-copper-binding analog Ctrl-CS3, in which the four metal-binding S atoms are replaced by isosteric carbons. Detailed synthesis is described in **Supplementary Note** and **Supplementary Figure 2a**. (b) Zn-limited and Zn-replete wild-type *C. reinhardtii* (CC-4532) cells were stained with the cuprous dye CS3 (ref. 25) to observe intracellular Cu distribution by confocal microscopy. As a control, we stained cells from the same cultures with the control dye Ctrl-CS3. DIC, differential interference contrast; Chl, chlorophyll autofluorescence. Scale bar, 10 μm. In total, we analyzed 55 Zn-deficient cells stained with CS3, 30 Zn-deficient cells treated with Ctrl-CS3, 54 Zn-replete cells stained with CS3 and 64 Zn-replete cells treated with Ctrl-CS3.

A key challenge for fluorescent probe design is to develop new reagents that enable live-sample detection of labile metal pools localized to particular subcellular compartments.

Mito-CS1 combines a BODIPY-based copper sensor with a triphenyl phosphonium moiety



MitoTracker Deep Red ; a commercially available mitochondrial tracker 17

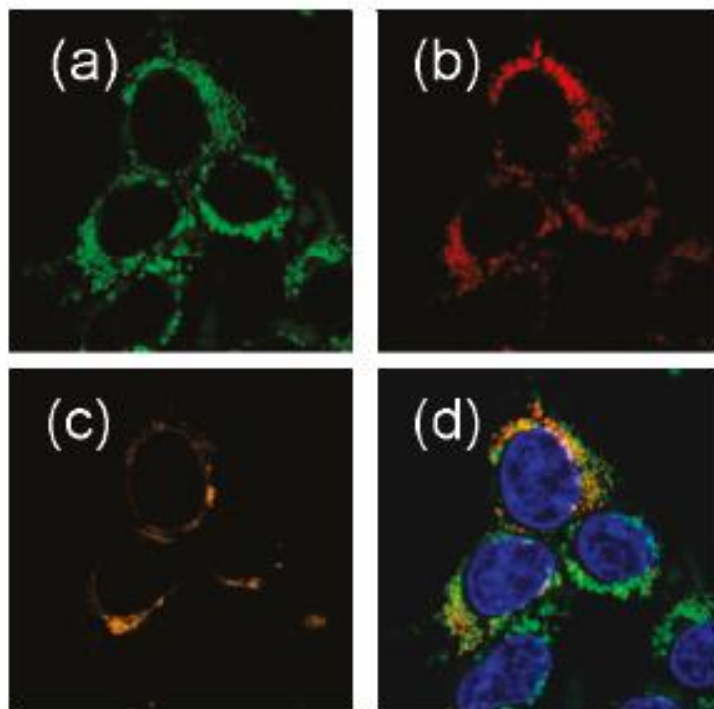
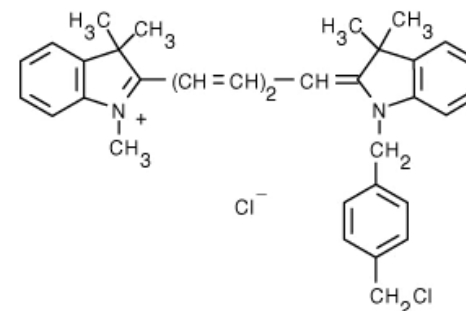
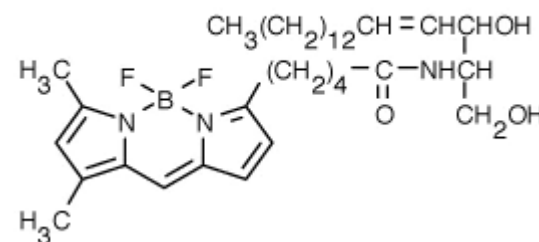


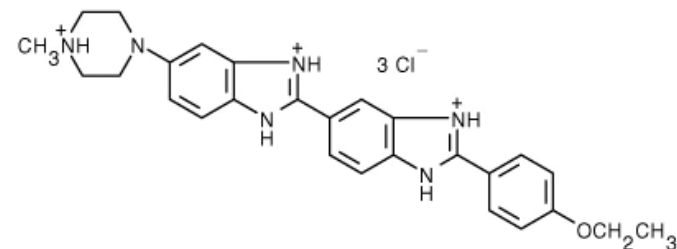
Figure 3. Mito-CS1 colocalizes to mitochondria in live HEK293T cells. HEK cells were stained with (a) 500 nM Mito-CS1, (b) 50 nM MitoTracker Deep Red, and (c) 2.25 μ M BODIPY FL C5-ceramide BSA complex and 5 μ M Hoechst 33342 for 15 min at 37 °C in DPB. (d) Overlay of (a) and (b) with Hoechst 33342.



BODIPY FL C5-ceramide ; a marker for the trans-Golgi



Hoechst 33342 ; nucleic acid stain



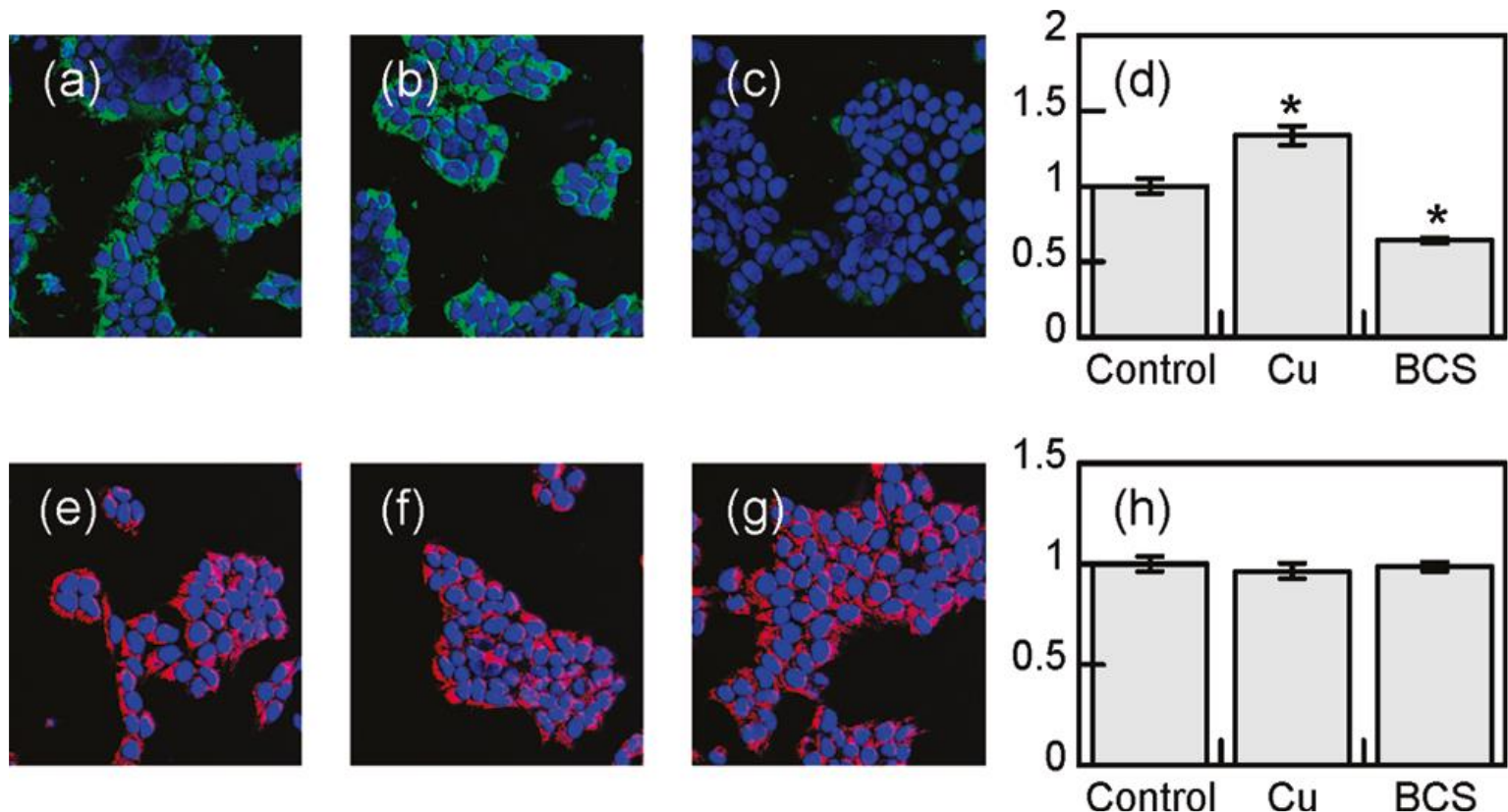
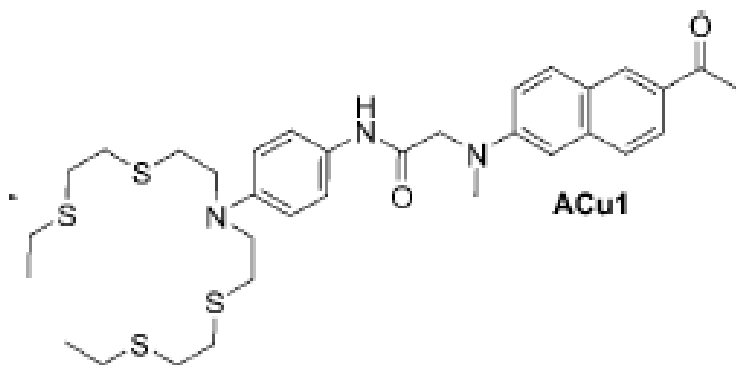


Figure 4. Live-cell molecular imaging with Mito-CS1 and Rhodamine 123 reveals a labile mitochondrial Cu^+ pool in HEK 293T Cells.

(a) Control HEK cells, (b) HEK cells supplemented with 300 μM CuCl_2 in the growth medium for 18 h at 37 C, and (c) HEK cells supplemented with 100 μM BCS in the growth medium for 18 h at 37 °C were stained with 500 nM Mito-CS1 and 5 μM Hoechst 33342 for 15 min at 37 °C in PBS. (d) Plot of the mean fluorescence intensity of (a)-(c). (e) Control HEK cells, (f) HEK cells supplemented with 300 μM CuCl_2 in the growth medium for 18 h at 37 °C, and (g) HEK cells supplemented with 100 μM BCS in the growth medium for 18 h at 37 °C were stained with 100 nM Rhodamine 123 and 5 μM Hoechst 33342 for 15 min at 37 C in DPBS. (h) Plot of the mean fluorescence intensity of (e)-(g)

Fluorescent probes with visible-wavelength excitation and emission profiles are useful for microscopy of cells, but visible light poorly penetrates tissue and whole animals.

For this reason, the development of fluorescent copper sensors with longer-wavelength, near-infrared excitation profiles has been targeted for these applications.



ACu1 ; a two-photon excitable probe with absorption of 750 nm

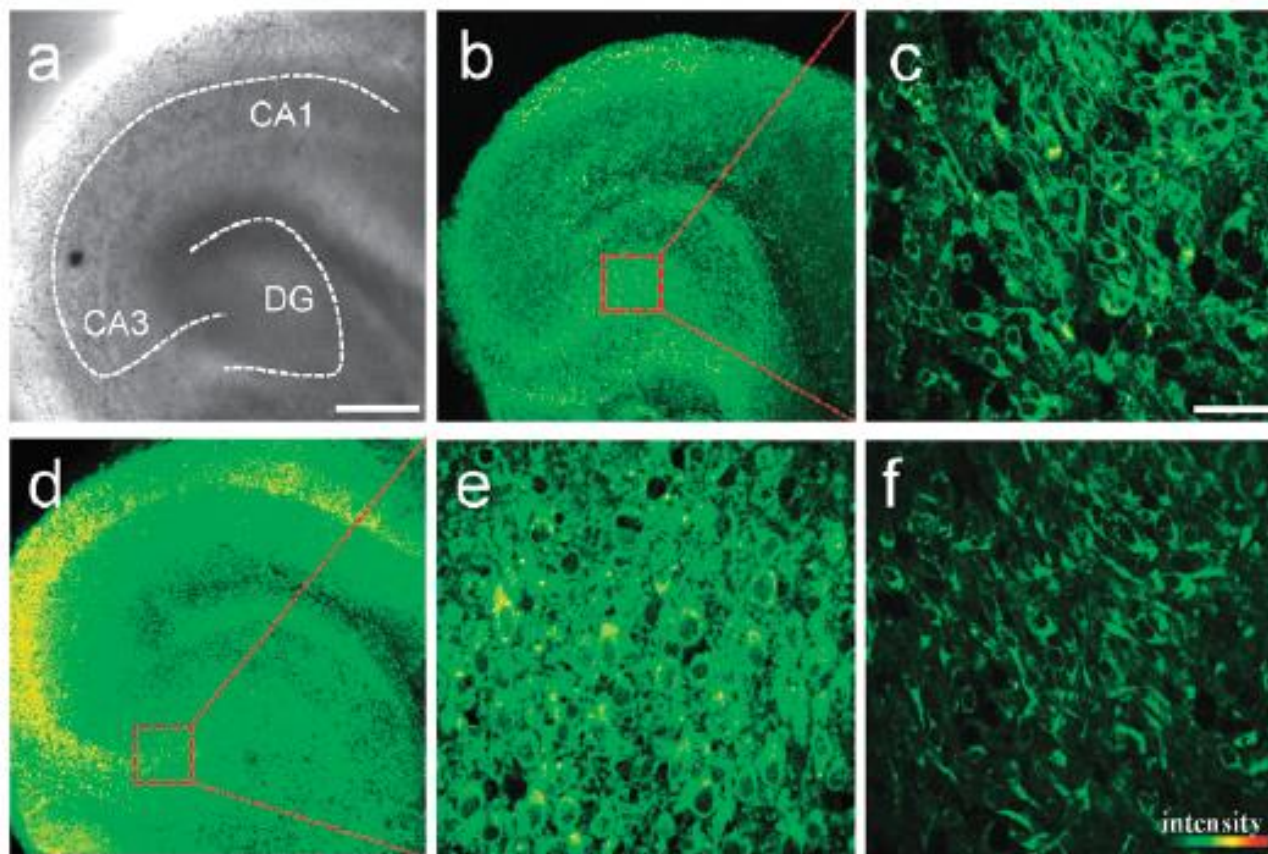
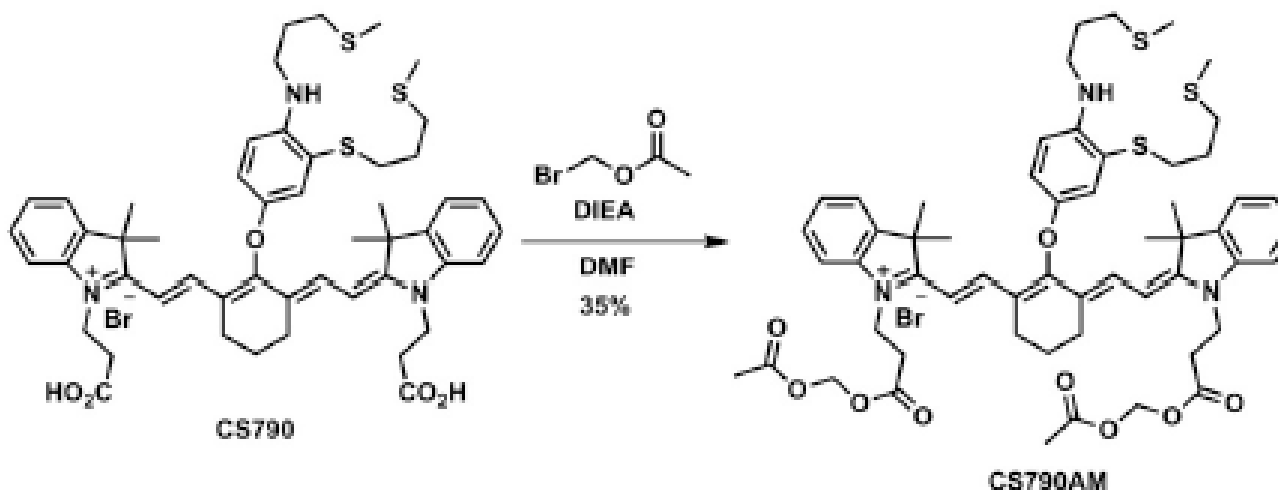


Fig. 4 Images of a fresh hippocampal slice of a 2-day old rat stained with 20 μM ACuI. (a) Bright-field image of CA1–CA3 regions as well as the dentate gyrus by 10 \times magnification. TPM image by 10 \times magnification of the slice that is (b) untreated and (d) pretreated with 1 mM CuCl_2 . 15 TPM images were accumulated along the z-direction at a depth of approximately 90–220 μm . Scale bar, 300 μm . (c,e) TPM image in the DG region (red box) of (b,d) at a depth of ~ 100 μm by magnification at 100 \times . Scale bar, 30 μm . (f) TPM image of (c) treated with 10 mM TAHD. The TPEF were collected at 400–620 nm upon excitation at 750 nm with a femtosecond pulse.



Coppersensor-790 (CS790) ;

near-infrared sensor based on a cyanine 7 fluorophore

The sensor features excitation at 760 nm and emission at 790 nm with pK_a value of < 2

CS790 displays about 15-fold turn-on response to Cu(I)

CS790AM ;

Greater membrane permeability and trapping in cell *via* de-esterification by intracellular esterases

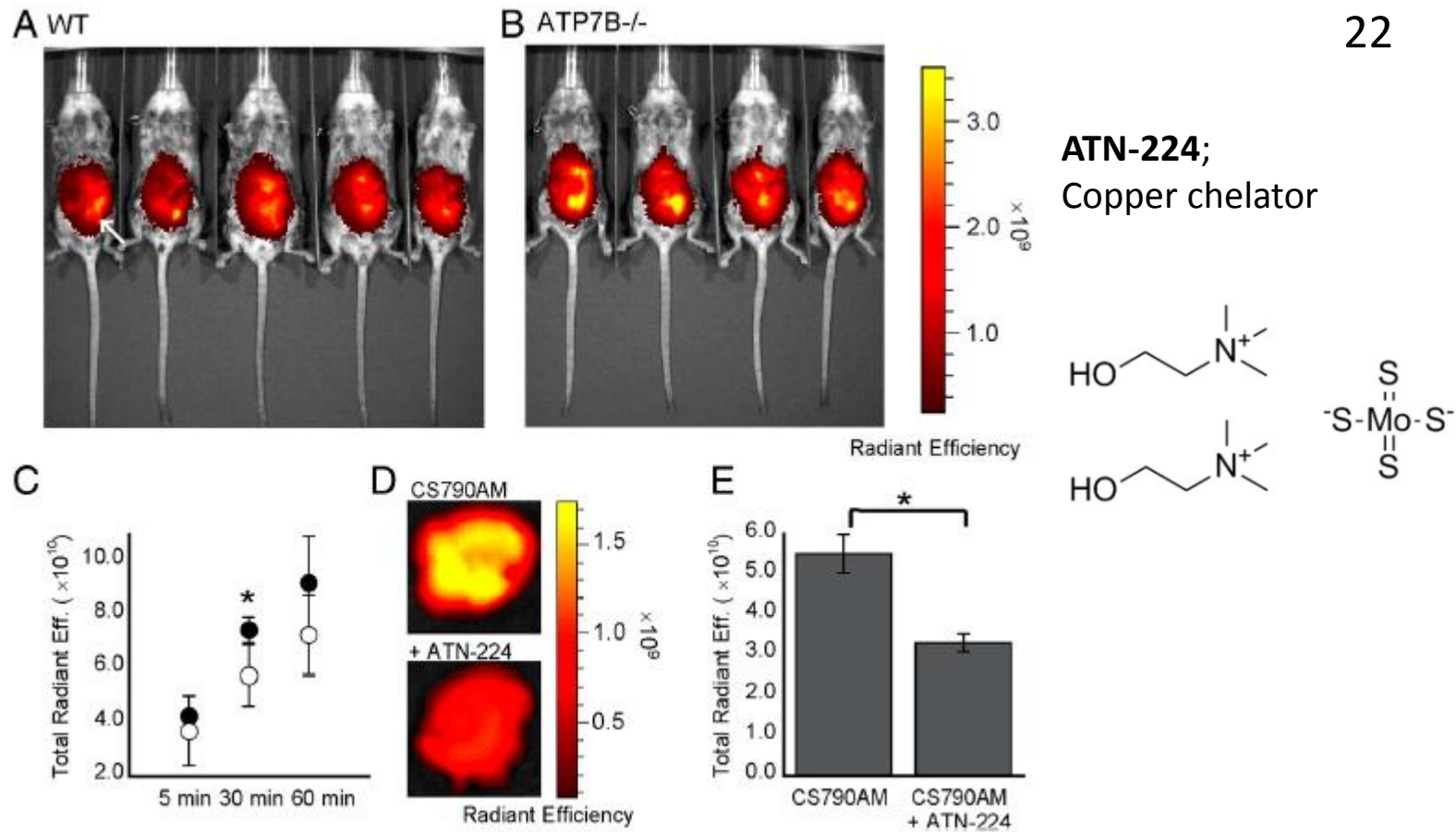
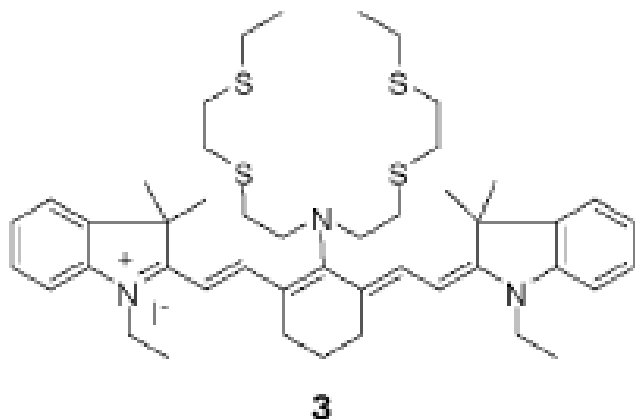


Fig. 5. CS790AM studies in *Atp7b*^{-/-} mice. (A and B) Images of WT (A) and *Atp7b*^{-/-} (B) mice 30 min after injection of CS790AM (0.1 mM, 50 μ L in 7:3 DMSO : PBS). White arrow indicates location of CS790AM injection site. (C) Plot of total fluorescent signal from *Atp7b*^{-/-} mice (black circles) and WT mice (white circles) 5, 30, and 60 min after CS790AM injection. (D) Representative images of livers from *Atp7b*^{-/-} mice injected with PBS (i.p., 50 μ L, Upper) or ATN-224 (i.p., 5 mg/kg in 50 μ L PBS, Lower) 2 h prior to CS790AM. (E) Total photon flux from imaged livers. Statistical analyses were performed with a two-tailed Student's *t*-test. **P* < 0.05 [*n* = 5 (A), *n* = 4 (B), *n* = 2 (D)] and error bars are \pm SD.



Probe 3 ;

Consisting of NS_4' coupled to directly to a cyanine fluorophore

This sensor has been applied to visualize ascorbic acid stimulated increases in labile Cu(I) in cells.

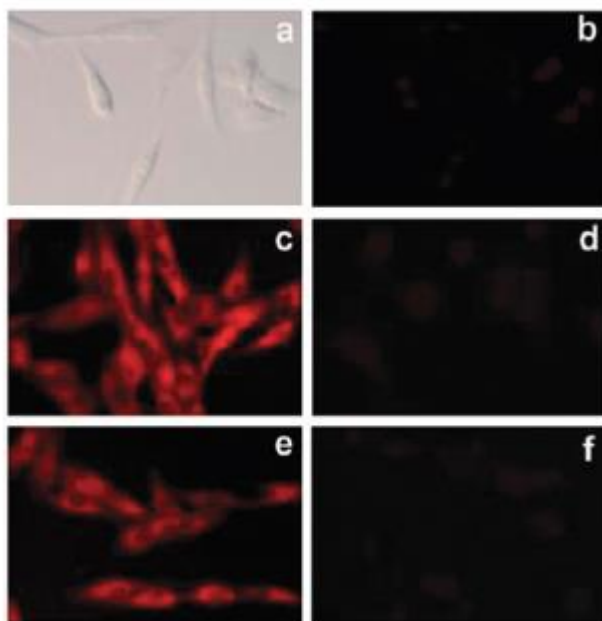
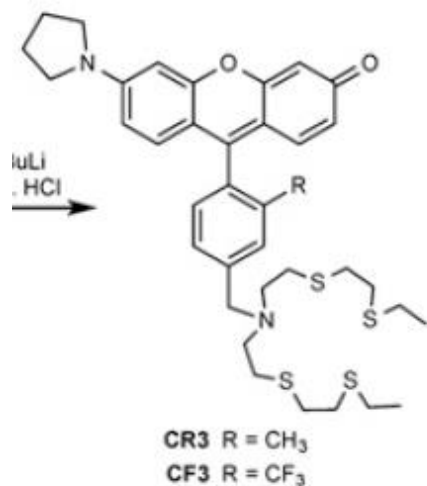
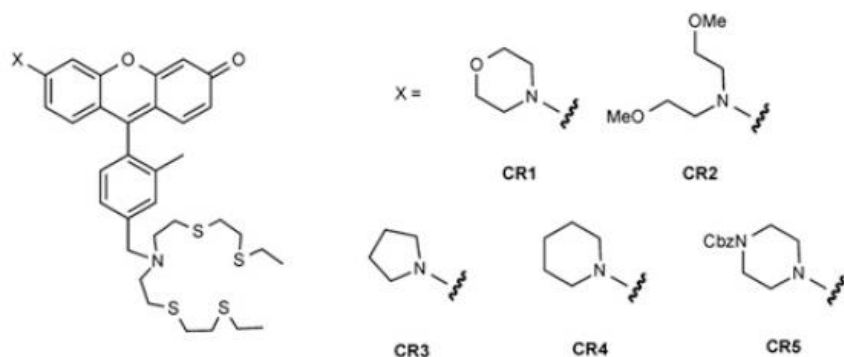


Fig. 3 Fluorescence and brightfield images of the living MG63 cells. (a) Brightfield image of the cells treated with the probe 3 (5 μM) for 10 min at 37 $^\circ\text{C}$; (b) fluorescence image of panel (a); (c) fluorescence image of the cells pretreated with CuCl_2 (200 μM) for 7 h and further incubated with the probe (5 μM) for 10 min at 37 $^\circ\text{C}$; (d) fluorescence image of the cells pretreated with CuCl_2 (200 μM) for 7 h, further incubated with probe (5 μM) for 10 min, and subsequently treated with the competing Cu^+ chelator BETA (50 μM) for an additional 10 min at 37 $^\circ\text{C}$; (e) fluorescence image of the cells pretreated with ascorbic acid (1 mM) for 4 h and then incubated with 5 μM probe 3 for 10 min at 37 $^\circ\text{C}$; (f) fluorescence image of the cells pretreated with ascorbic acid (1 mM) for 4 h, further incubated with 5 μM probe 3 for 10 min, and subsequently treated with the competing Cu^+ chelator BETA (50 μM) for an additional 10 min at 37 $^\circ\text{C}$.

Although useful in many settings, BODIPY sensors were limited in some cases by their high hydrophobicity, insufficient photostability.

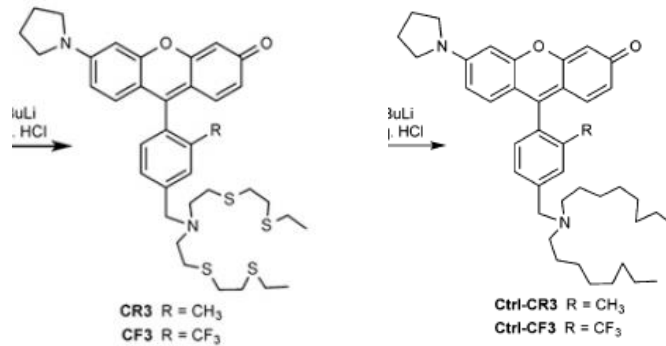


Copper Rhodol 3 (CR3) ;

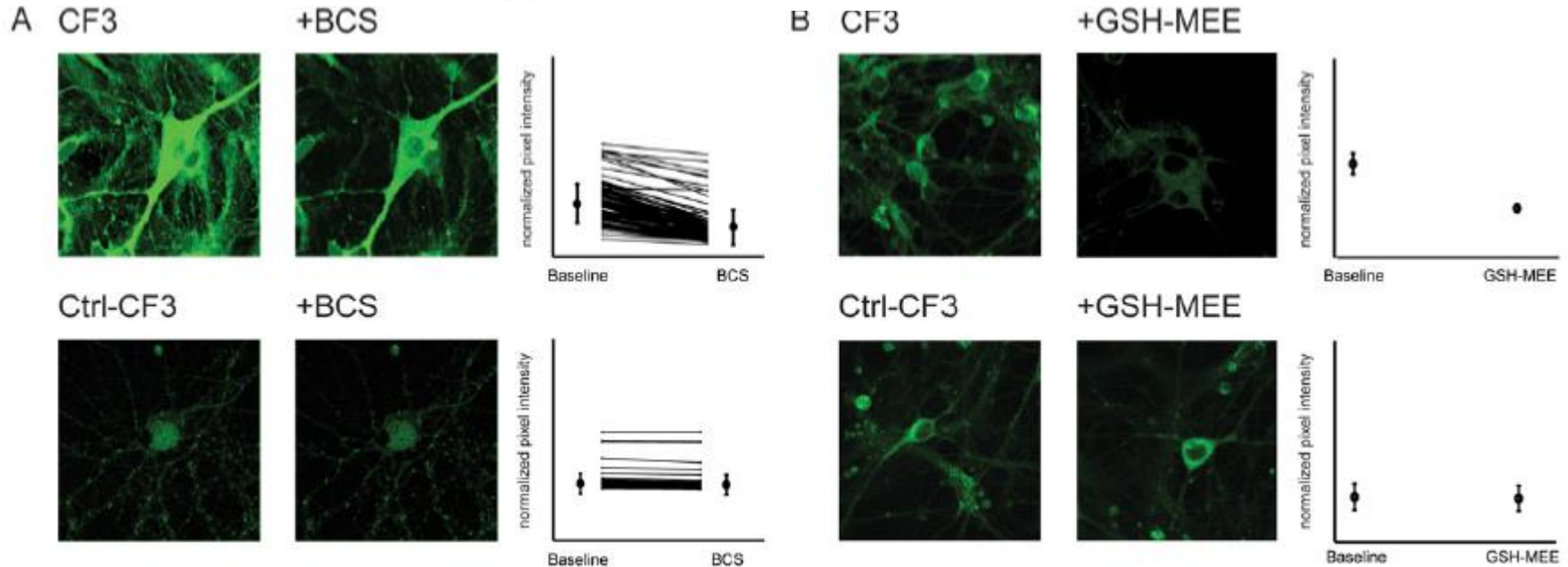
Of the five initial targets, CR3 was the best performing dye exhibiting a 13-fold turn-on response to Cu(I)

Copper Fluor-3 (CF3) ;

The substitution of a methyl group on the aryl ring with a more bulky trifluoromethyl group



Proc. Natl. Acad. Sci. U. S. A., **2014**, *111*, 16280–16285.

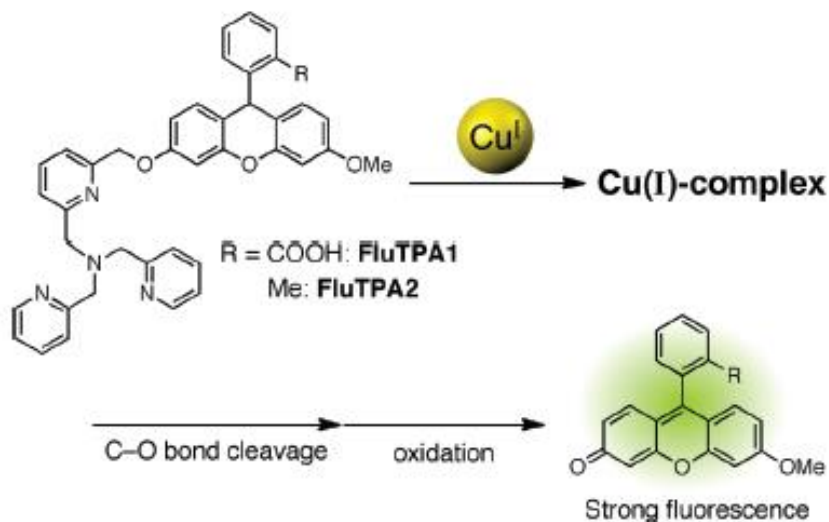


(A) Live-cell confocal imaging with CF3 and Ctrl-CF3 in dissociated hippocampal neurons suggests that acute BCS treatment alters intracellular labile Cu⁺. Representative images are shown of hippocampal neurons that were incubated with 2 μM of the copper-responsive CF3 dye or Ctrl-CF3, which does not respond to copper, for 20 min. Fluorescence before and followed by 30 min of BCS perfusion were compared.

(B) CF3 staining of dissociated hippocampal neurons treated with GSHMEE suggests that CF3 can respond to changes in the GSH-dependent copper pool. (Top) Representative images of hippocampal neurons stained with CF3 with and without GSH-MEE treatment (control n = 6 cultures, GSH-MEE n = 6 cultures). (Bottom) Representative images of hippocampal neurons stained with Ctrl-CF3 with and without GSH-MEE treatment show that this dye does not respond to changes in the GSH-dependent copper pool (control n = 7 cultures, GSH-MEE n = 7 cultures).

Reaction-based fluorescent probes

Alternative strategy to probe biological copper is to exploit reaction, rather than reversible recognition.



FluTPA1 ;

The first reaction-based sensor for Cu(I) with O₂

Combining a reduced fluorescein-type dye capped with a tetradentate tris[(2-pyridyl)-methyl]amine (TPA) ligand for copper.

Upon Cu(I) binding and reaction under aerobic conditions, the benzyl ether C-O bond is cleaved and oxidation liberates fluorescein.

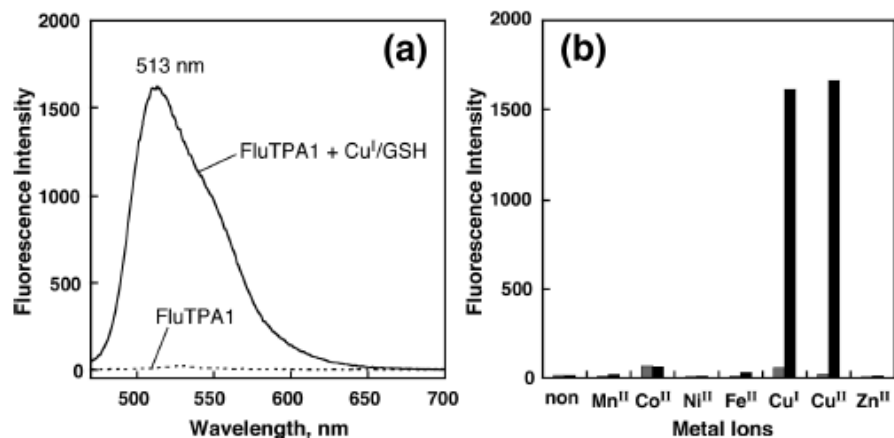


Figure 1. (a) Fluorescence response of 1 μM FluTPA1 before (dotted line) and after (solid line) reaction with 20 μM $[\text{Cu}^{\text{I}}(\text{CH}_3\text{CN})_4]\text{PF}_6$. The solid spectrum was recorded after 2 h of reaction of FluTPA1 with Cu^{I} in 50 mM HEPES (pH 7.20) containing 2 mM glutathione (GSH). The excitation wavelength was 470 nm. (b) Metal ion selectivity of FluTPA1 in 50 mM HEPES buffer (pH 7.20). The bars represent the fluorescence intensity at 513 nm after 2 h of reaction of 1 μM FluTPA1 with each type of metal ion (20 μM) in the absence (gray bars) or presence (black bars) of 2 mM GSH.

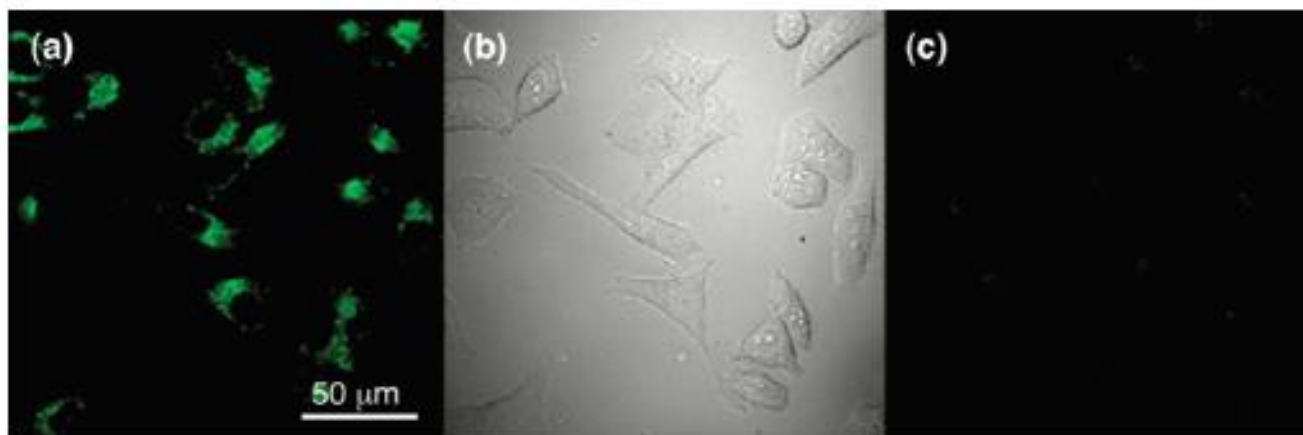
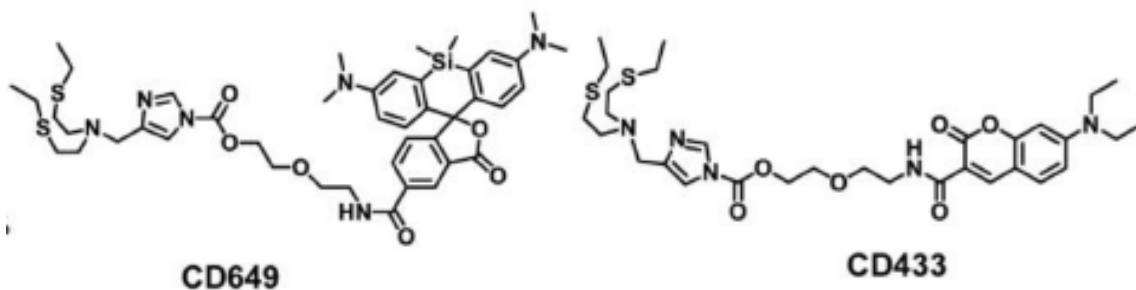
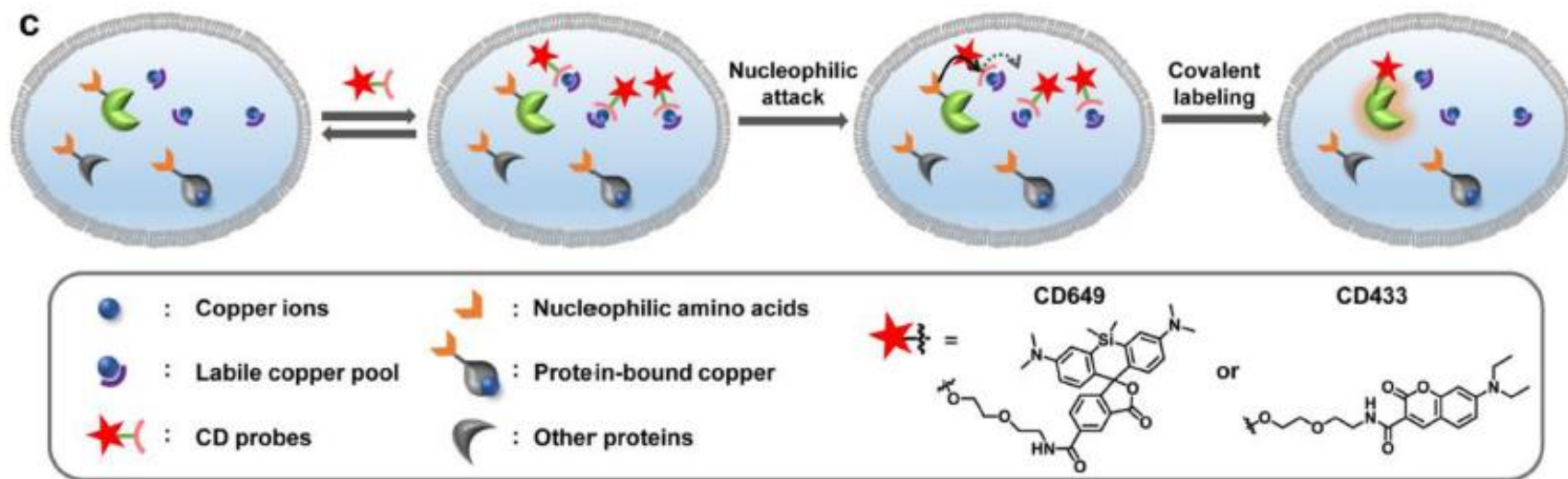


Figure 2. (a) Confocal fluorescence image of HeLa cells supplemented with 100 μM CuCl_2 for 8 h and then further incubated with 5 μM FluTPA2 for 3 h at 37 $^\circ\text{C}$. (b) Bright-field transmission image of the cells shown in (a). (c) Confocal fluorescence image of FluTPA2-loaded cells grown in a basal medium.

Recent research

Activity-based fluorescent probes

Fluorescent copper detection using acyl imidazole bioconjugation chemistry



Probes that feature a thioether NS2 receptor bearing a fused acyl imidazole linked to coumarin or Si-rhodamine

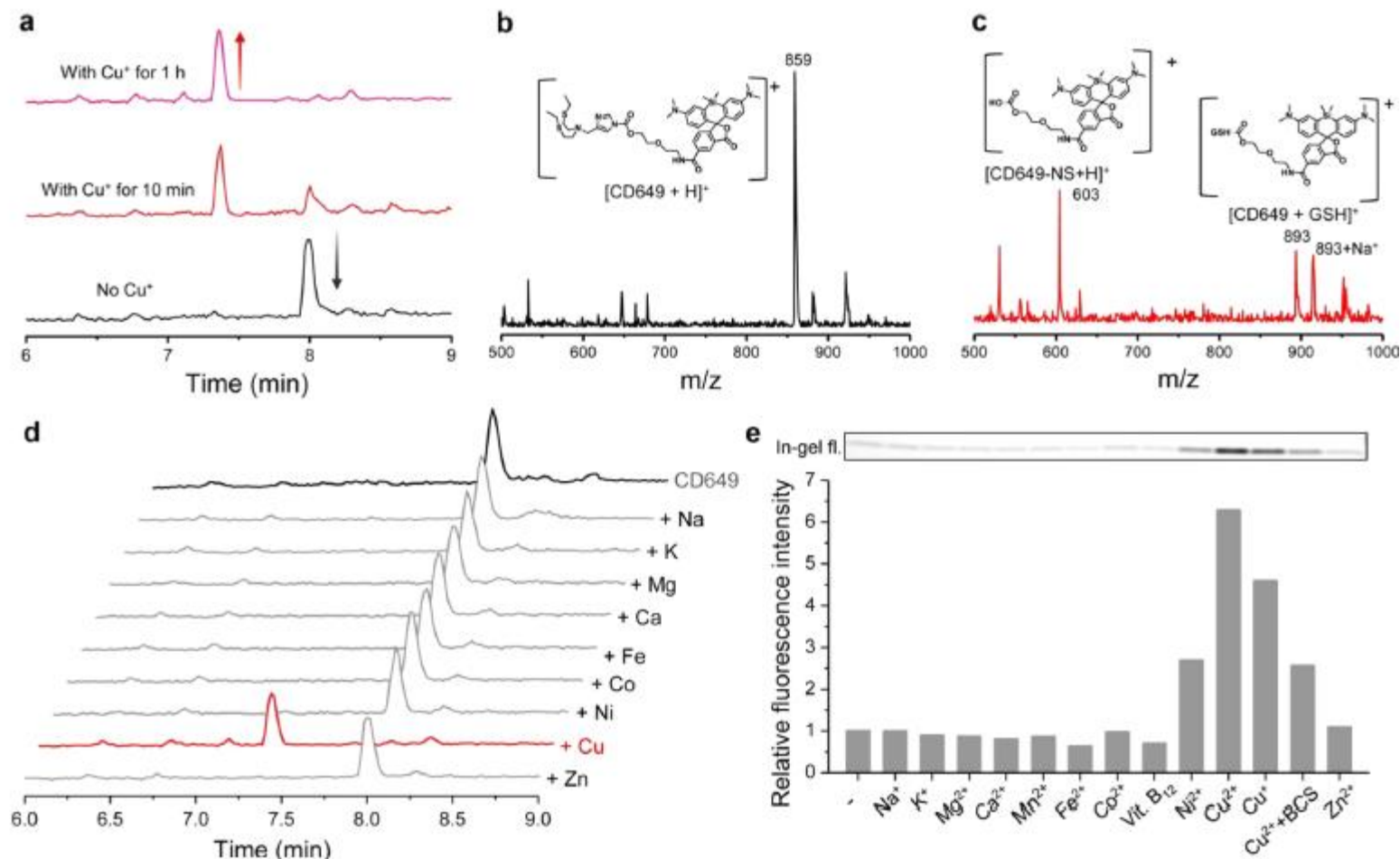


Figure 1. Copper reactivity and selectivity of CD probes in aqueous buffer solutions. (a) LC chromatograms of the reaction between 5 μ M CD649 and 10 μ M Cu(I) in PBS containing 25 μ M L-serine methyl ester and 2 mM GSH for 1 h, showing the complete conversion of CD649. (b) The mass of intact CD649 probe was detected at a retention time of 8.0 min in the absence of Cu(I). (c) The copper-responsive reaction products of CD649 with Cu(I)/2 mM GSH are detected at a retention time of 7.4 min. (d) LC chromatograms of 5 μ M CD649 (top trace, black), 5 μ M CD649 incubated with 10 μ M Cu(I) (red trace) for 30 min, and other biologically relevant metals at 10 μ M (Na⁺, K⁺, Mg²⁺, Ca²⁺, Fe³⁺, Co²⁺, Ni²⁺, Cu⁺, and Zn²⁺, gray traces) for 30 min in PBS in the presence of 25 μ M L-serine methyl ester and 2 mM GSH. The LC data support that CD649 shows high selective reactivity toward copper ions. (e) In-gel fluorescence images and integrated fluorescence intensities of CD649 and lysozyme as a model protein for activity-based sensing of copper via copper-induced bioconjugation. Lysozyme was preincubated with biologically relevant metal ions for 5 min (s-block metal ions at 1 mM, d-block metal ions at 10 μ M, BCS at 50 μ M), followed by incubation with 1 μ M CD649 at room temperature for 2 h. In-gel fluorescence for SDS-PAGE was scanned by ChemiDoc MP and signal intensity was analyzed by ImageJ.

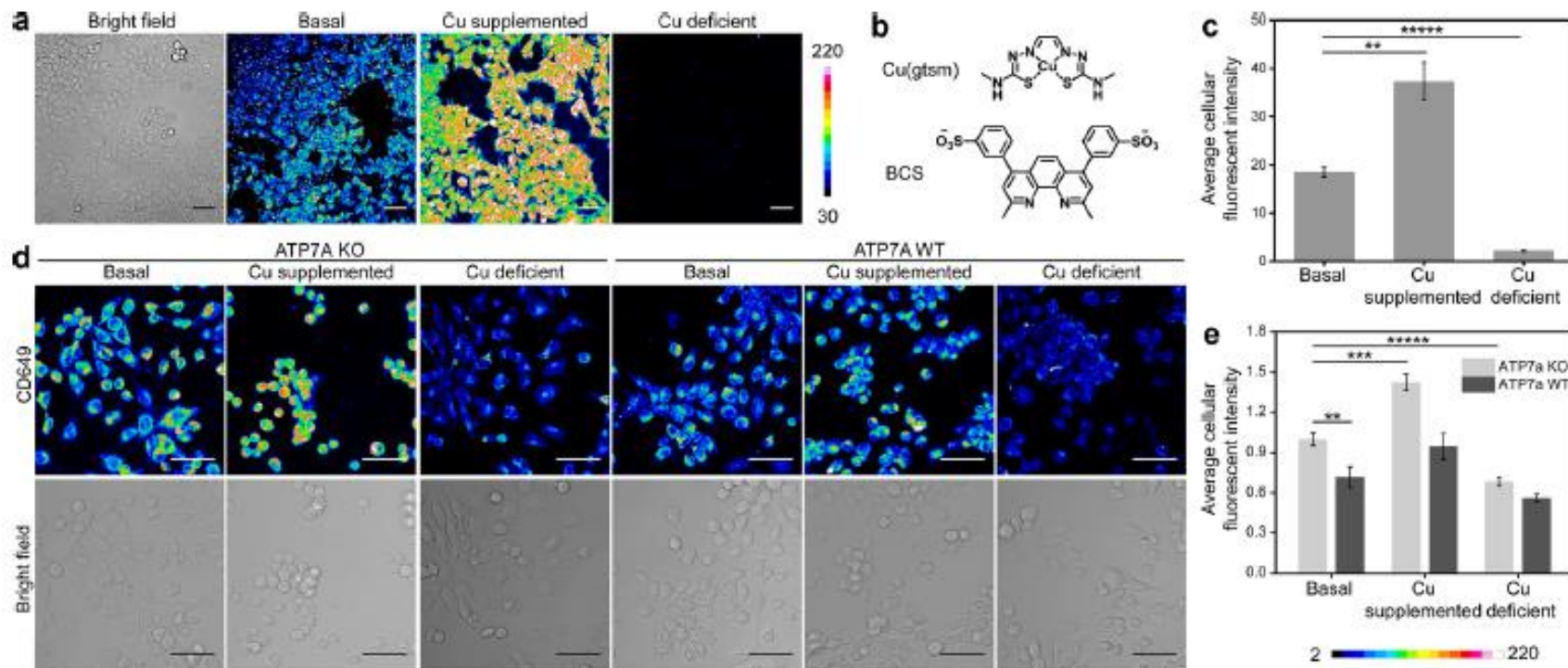


Figure 2. Fluorescence imaging of labile copper pools in live HEK293T cells and MEF cells with wild-type or altered expression levels of the copper transporter protein ATP7A using CD649. (a) Confocal fluorescence microscopic images of HEK 293T cells treated with 1 μ M CD649 alone, CD649 and 2 μ M Cu(gtsm) for Cu supplementation, or CD649 and 200 μ M BCS for Cu deficiency. The cells were incubated with 2 μ M Cu(gtsm) for 2 h or 200 μ M BCS in DMEM/10% FBS medium overnight and washed with DMEM/10% FBS and PBS, followed by incubation with 1 μ M CD649 in DPBS solution and then imaged after 15 min. (b) Chemical structures of Cu(gtsm) and BCS. (c) Normalized cellular fluorescence intensities of the HEK 293T cells as determined using ImageJ, showing a turn-on response when treated with Cu(gtsm) and a turn-off response in the presence of BCS. Error bars denote standard derivation (SD; $n = 3$). Scale bar = 50 μ m. (d) Confocal fluorescence microscopic images of MEF ATP7A WT or KO cells treated with DMSO vehicle, 2 μ M Cu(gtsm) for 30 min, or 200 μ M BCS for overnight in DMEM/10% FBS and washed with DMEM/10% FBS and PBS, followed by incubation with 1 μ M CD649 in DPBS and then imaged after 15 min. (e) Average cellular fluorescence intensity of CD649 determined from experiments performed in triplicate with $\lambda_{ex} = 633$ nm. Error bars denote standard derivation (SD; $n = 3$). Scale bar = 50 μ m. * $p < 0.05$, ** $p < 0.01$, *** $p < 0.001$, and **** $p < 0.0001$.

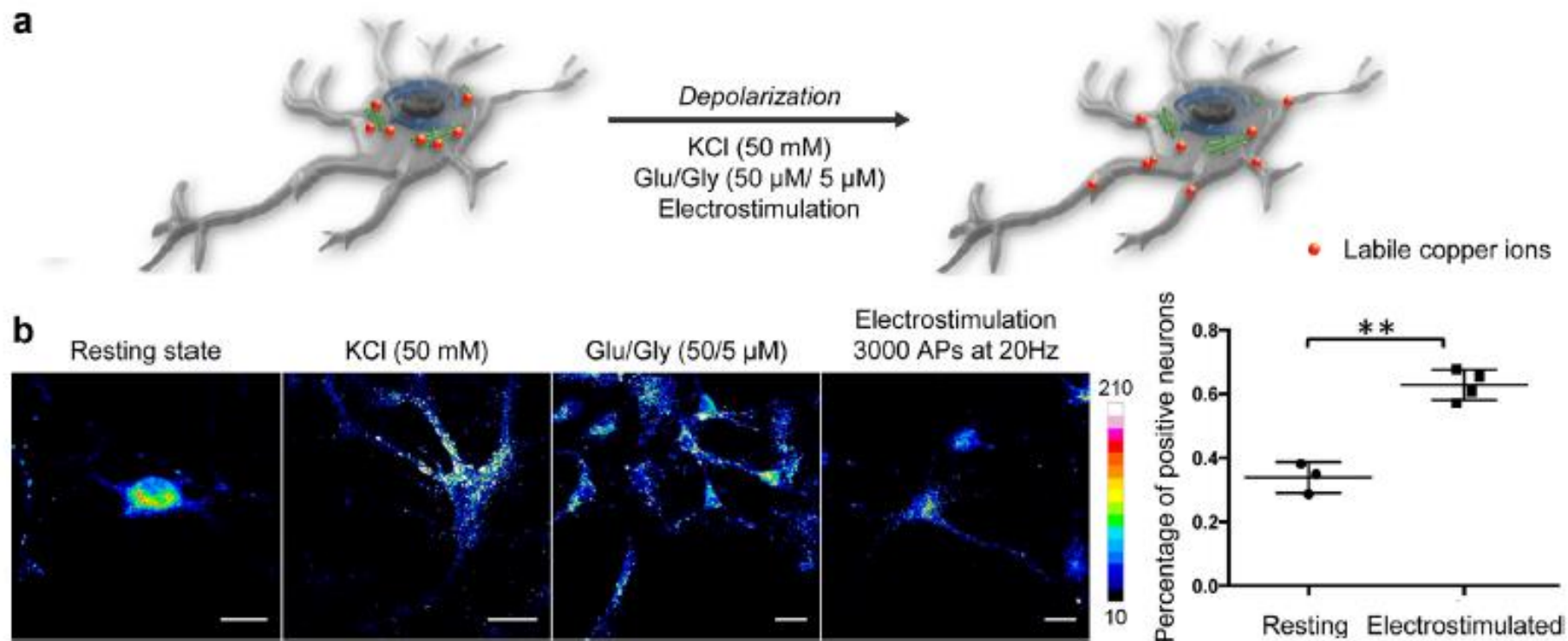


Figure 3. CD649 can image translocation of labile copper pools from cell bodies to projections in cultured primary neurons upon chemical/electrical stimulation. (a) Depiction of observed copper redistributions in neurons before and after depolarization by various stimuli. (b) Fluorescence images of primary cultured hippocampal neurons stained with 1 μ M CD649 in the resting state and after depolarization by KCl (50 mM), 50 μ M glutamate and 5 μ M glycine (Glu/Gly), or electrostimulation (3000 evoked action potentials at a frequency of 20 Hz). (c) Percentage of neurons showing copper pools residing at distances greater than one cell body away from soma. The percentage of such neurons increases significantly after depolarization. Scale bar is 20 μ m. ** $p < 0.01$.

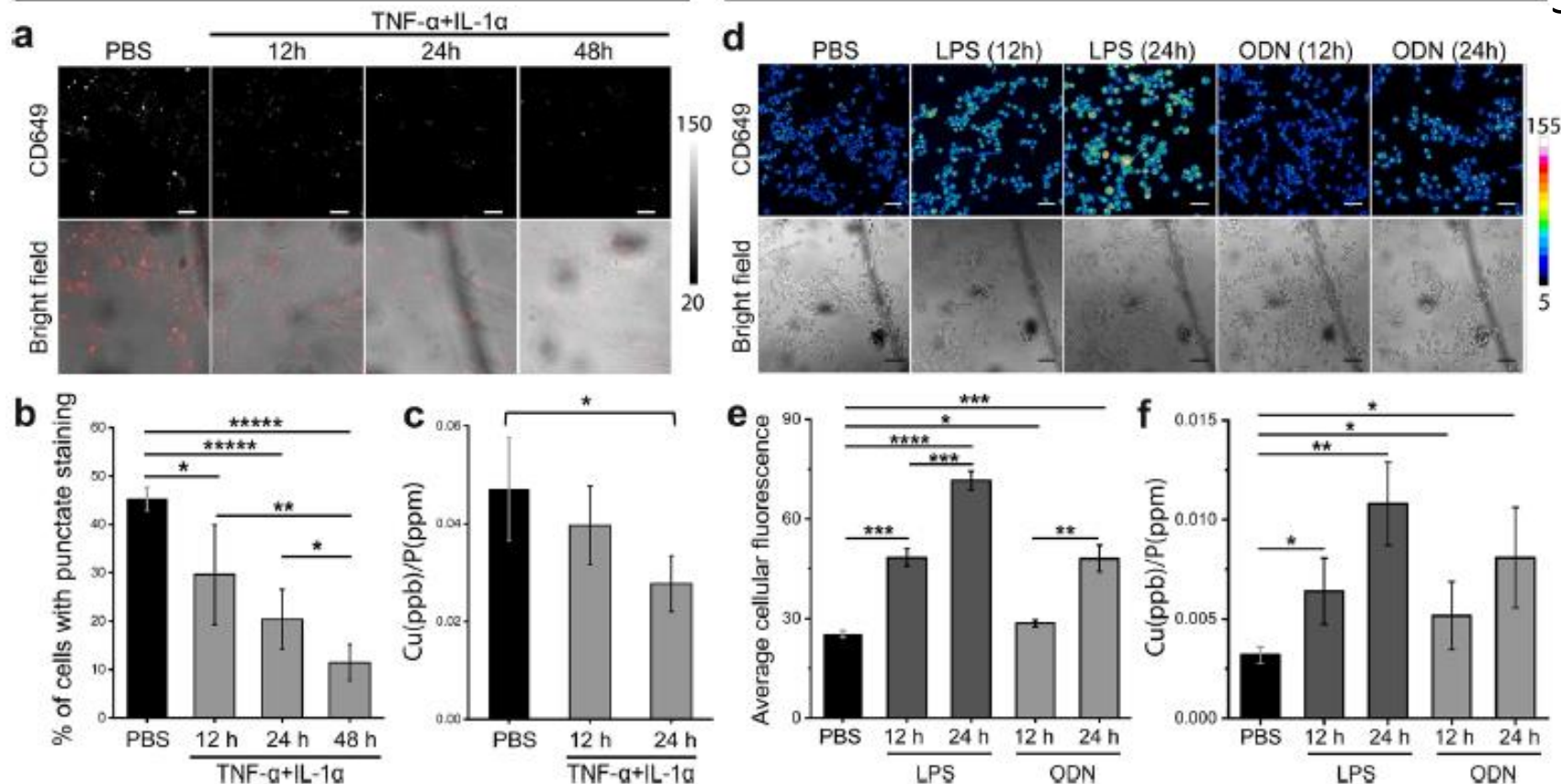


Figure 4. Fluorescence imaging of labile copper pools in human astrocytes (HA) and microglia SIMA9 under various inflammatory responses using CD649. (a) Confocal fluorescence microscopic images of astrocytes treated by PBS control or a combination of TNF- α and IL-1 α (both at 20 ng/mL) up to 48 h and stained with 5 μM CD649 in HBSS for 30 min, fixed and then imaged. Scale bar = 25 μm . (b) Average cellular fluorescence intensity of CD649 determined from experiments in (a) performed in triplicate with $\lambda_{\text{ex}} = 633$ nm. Error bars denote standard deviation (SD; $n = 3$) (c) ICP-MS measurement to determine total cellular ^{63}Cu levels in astrocytes under TNF- α and IL-1 α inflammatory stimuli (with normalization of different cell numbers by total cellular ^{31}P level). Error bars denote SD; $n = 2$. (d) Confocal fluorescence microscopic images of microglia stimulated by PBS control, lipopolysaccharide (LPS, 0.1 $\mu\text{g}/\text{mL}$), or CpG oligodeoxynucleotides (ODN, 5 $\mu\text{g}/\text{mL}$). Five μM CD649 in HBSS was incubated subsequently for 30 min and then imaged after fixation. Scale bar = 25 μm . (e) Average cellular fluorescence intensity of CD649 determined from experiments in (d) performed in triplicate with $\lambda_{\text{ex}} = 633$ nm. Error bars denote SD; $n = 5$ different images from the triplicate experiments. (f) ICP-MS measurement to determine total cellular ^{63}Cu levels in microglia under various inflammatory stimuli (with normalization of different cell numbers by total cellular ^{31}P level). Error bars denote SD; $n = 2$. * $p < 0.05$, ** $p < 0.01$, *** $p < 0.001$, and **** $p < 0.0001$.

-
- Fluorescent chemical probes offer a powerful set of reagents for probing the biology of copper as an essential element for life.
 - Most fluorescent copper probes are designed to recognize labile copper ions based on thioether-rich receptors or TPA receptors.
 - Recently fluorescent copper probe using acyl imidazole bioconjugation chemistry was reported.
 - The synthetic chemistry and technology development for Cu(I) probes is still in early stage compared to broadly-useful fluorescent indicators for Ca(II) and Zn(II), so a number of exciting possibilities remain open.

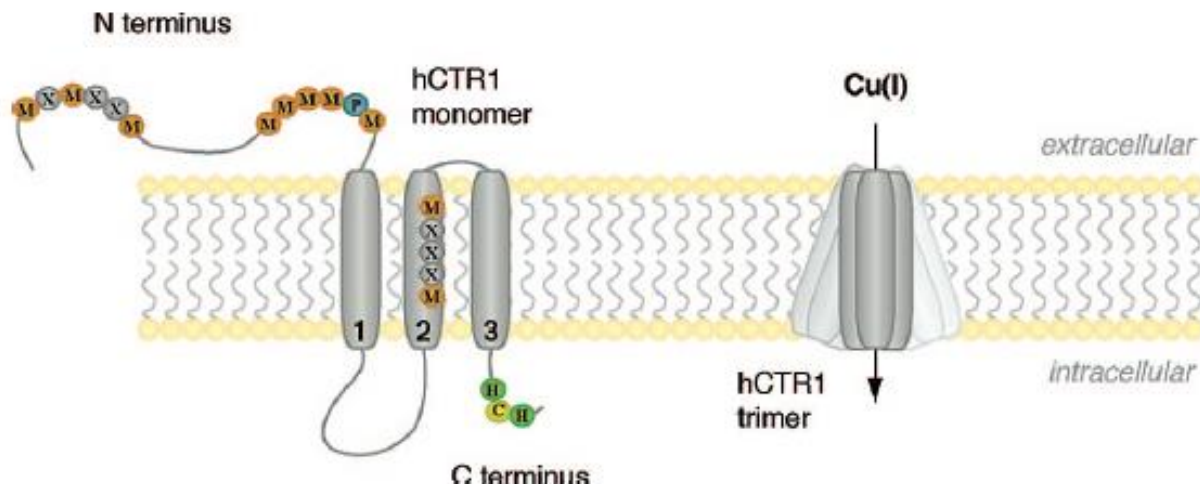


Figure 2. Overall architecture of hCtr1.

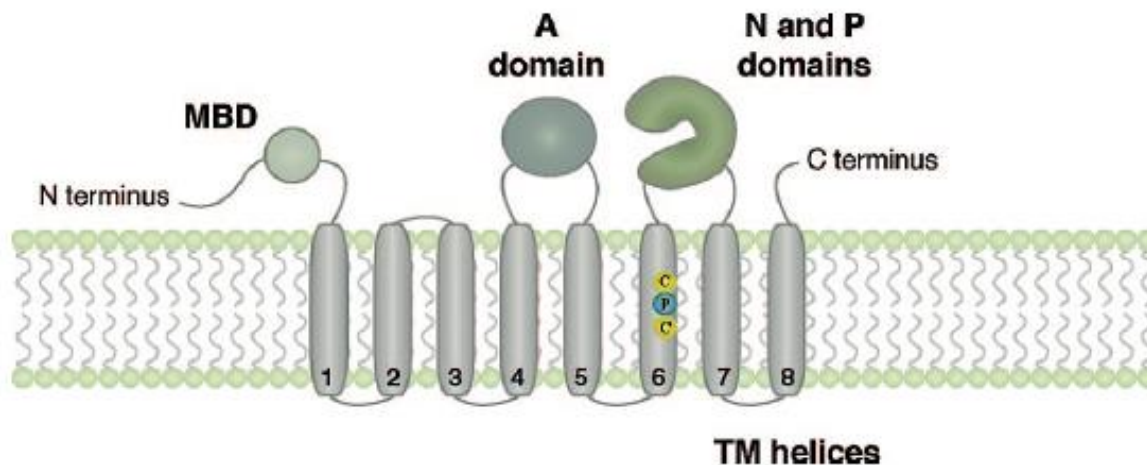


Figure 3. Overall architecture of Cu(I) P_{1B}-type ATPases. The number of MBDs at the N-terminus ranges from one to six, depending on the organism.

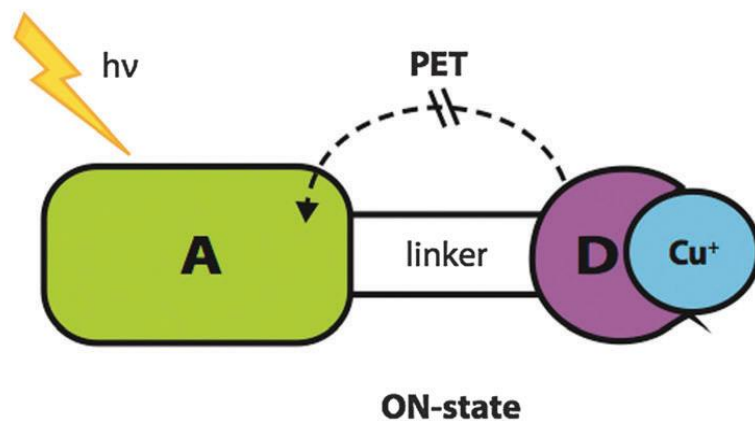
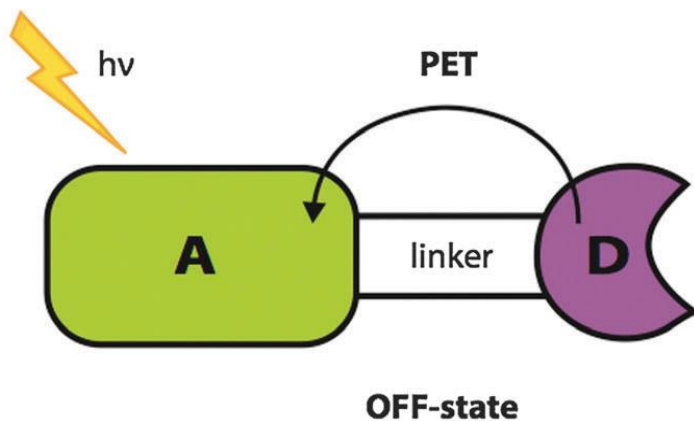
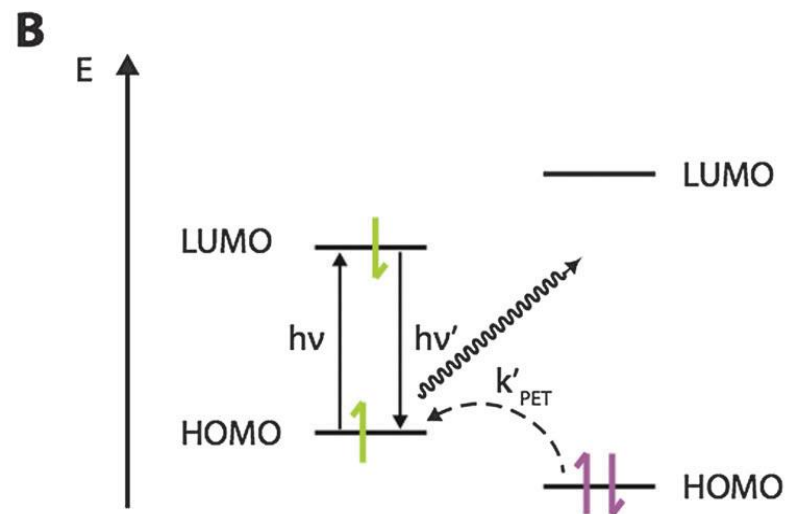
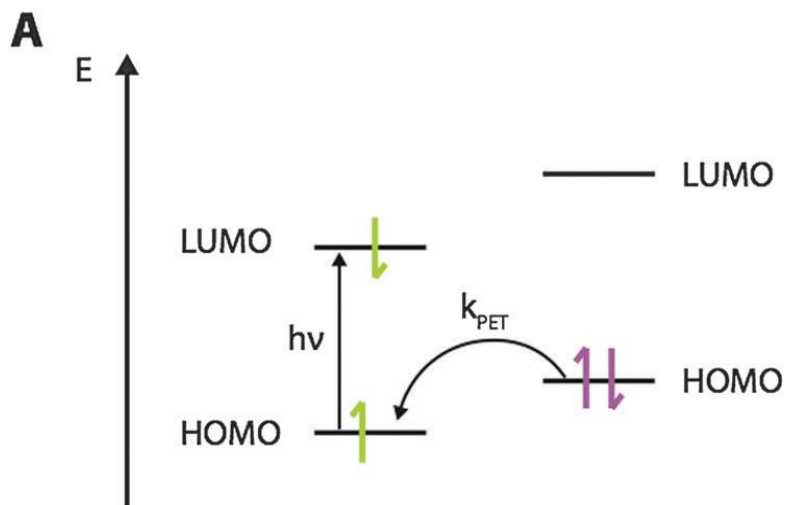
Table 1 Apparent dissociation constants for Cu(I)-binding proteins and small-molecule ligands

Protein/ligand	K_d^a (fM)
Atox1	16.8
ATP7A (Menkes)	
MBD1 ^b	2.5
MBD2	4.9
MBD3	104
MBD5	13.0
MBD6	2.6
CCS ^c	2.4
SOD1 Cu site	0.23
MT-2 ^d	0.41
GSH	9130
Dithiothreitol (DTT)	7940 ^e

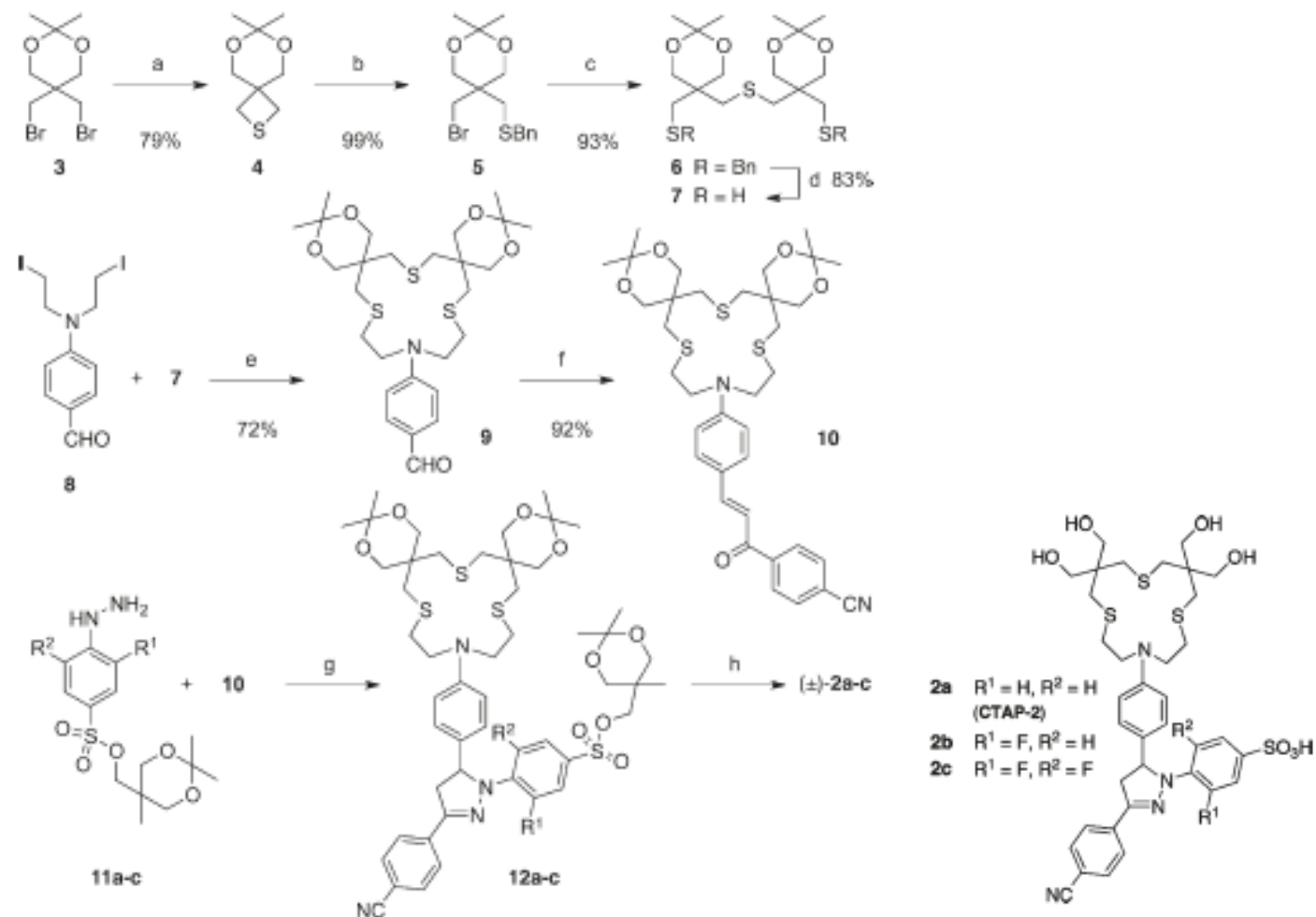
^a Ref. 64. ^b MBD: metal binding domain. ^c CCS: copper chaperone for Cu,Zn superoxide dismutase (SOD1). ^d MT-2: Metallothionein 2. ^e Ref. 71.

Design principles for developing Cu(I) sensors of biological utility

36

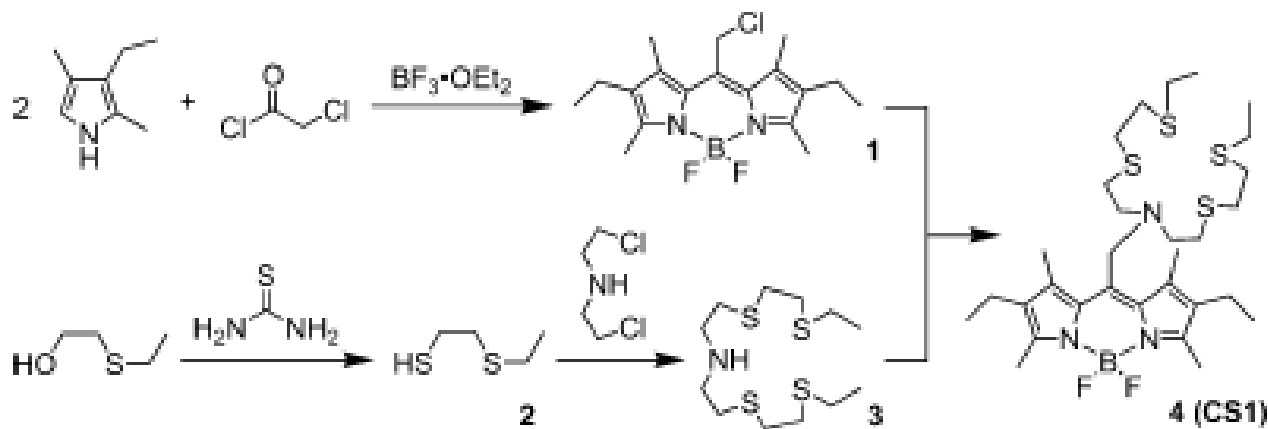


Scheme 1. Synthesis of Pyrazoline Probes 2a–c^a



^a Reagents and conditions: (a) Na₂S·9H₂O, KI, MeOH–H₂O; (b) BnBr, K₂CO₃, CH₃CN; (c) Na₂S·9H₂O, KI, DMF–H₂O; (d) Na, NH₃(l), THF; (e) Cs₂CO₃, DMF; (f) 4-acetylbenzonitrile, pyrrolidine, C₆H₆–EtOH; (g) PPTS, pyridine; (h) TFA–H₂O (9:1), ^tBuOH–THF, KO^tBu.

Scheme 1. Synthesis of Coppersensor-1 (CS1)



The synthesis of CS1 is outlined in Scheme 1.

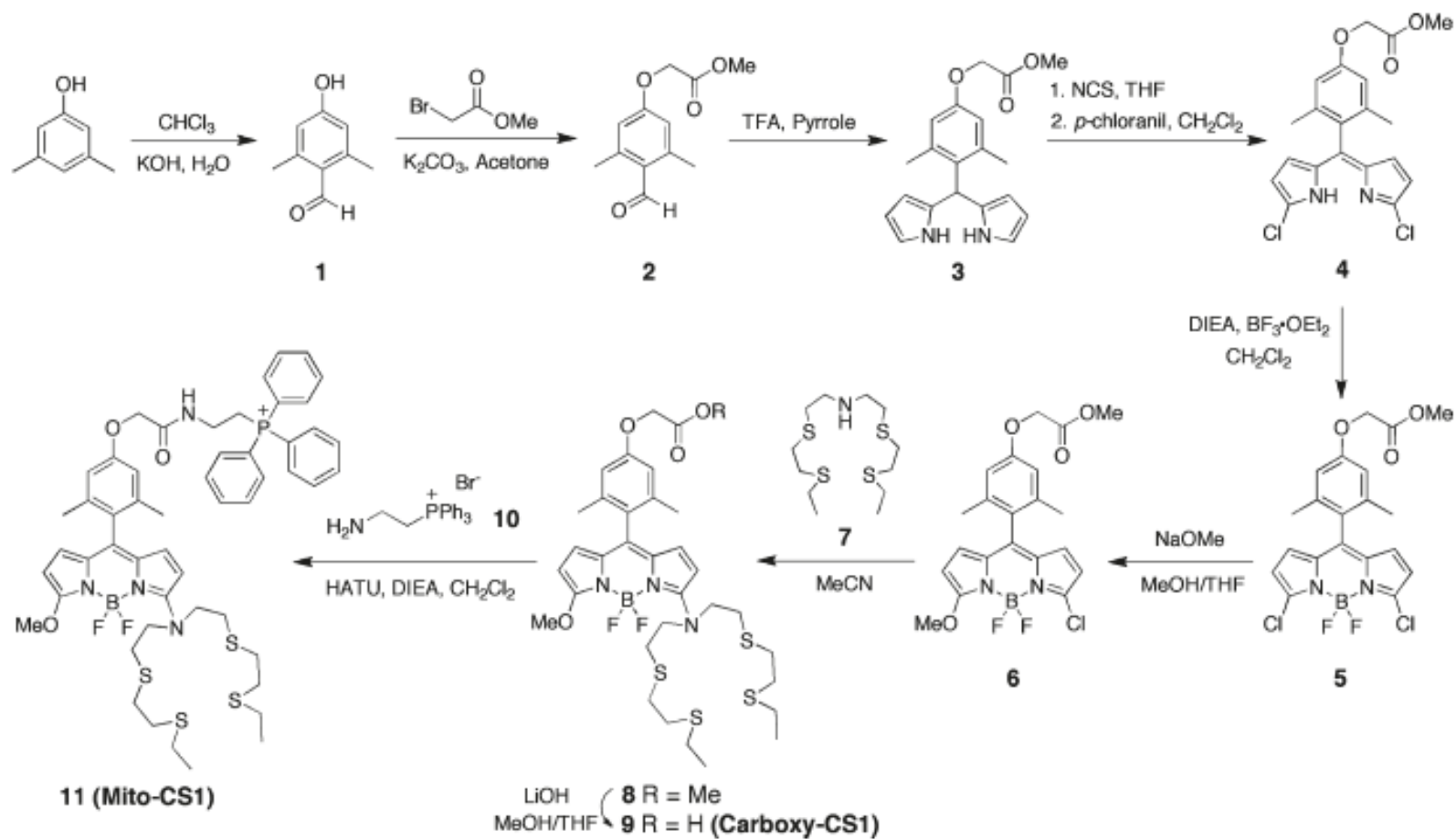
BODIPY **1** is obtained in a one-pot, two-step procedure via condensation of 2,4-dimethyl-3-ethylpyrrole with chloroacetyl chloride followed by treatment with $\text{BF}_3 \cdot \text{OEt}_2$. The overall yield is 16% for two steps.

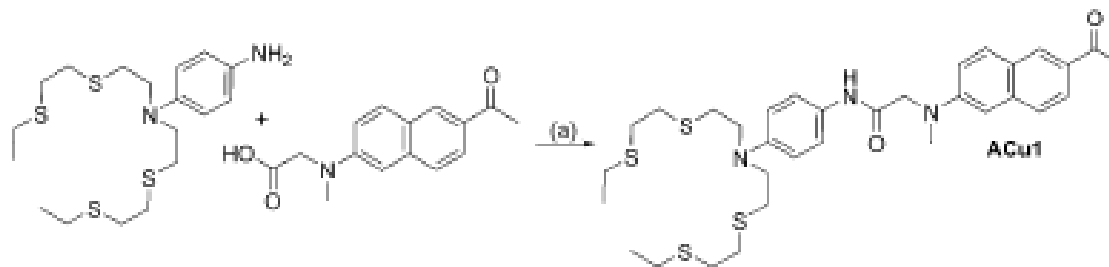
The tetrathia receptor **3** is also delivered in two steps. Conversion of ethyl 2-hydroxyethyl sulfide with thiourea and HBr proceeds smoothly to generate thiol **2** in 84% yield.

Treatment of **2** with bis(2-chloroethyl)amine hydrochloride under basic conditions furnishes the azatetrathia receptor **3** in 79% yield.

Coupling of **1** and **3** in refluxing acetonitrile affords CS1 (**4**) in 22% yield after workup and purification.

Scheme 1





Scheme 1 Synthesis of ACuI. (a) DCC, HOBt, CH₂Cl₂.

Chem. Commun., **2011**, 47, 7146–7148.

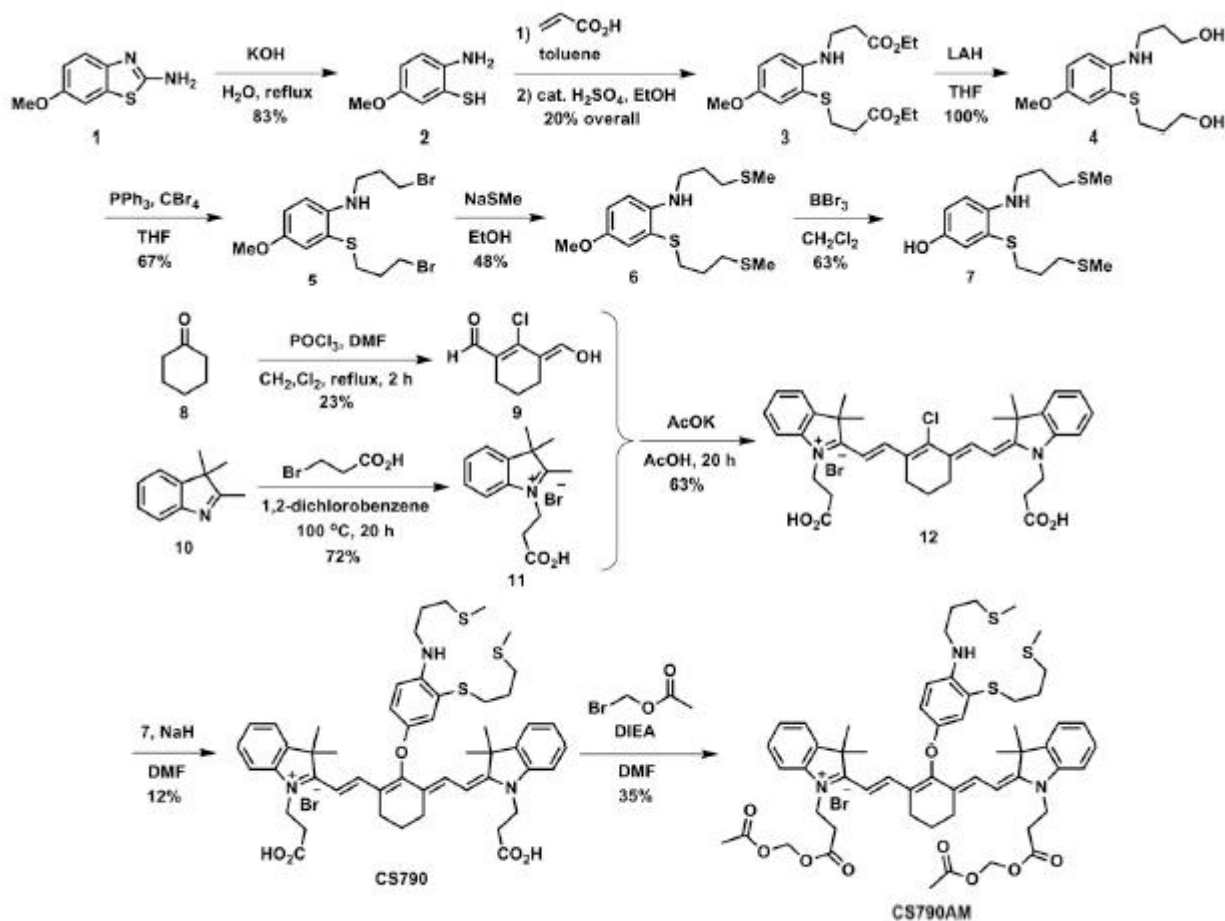
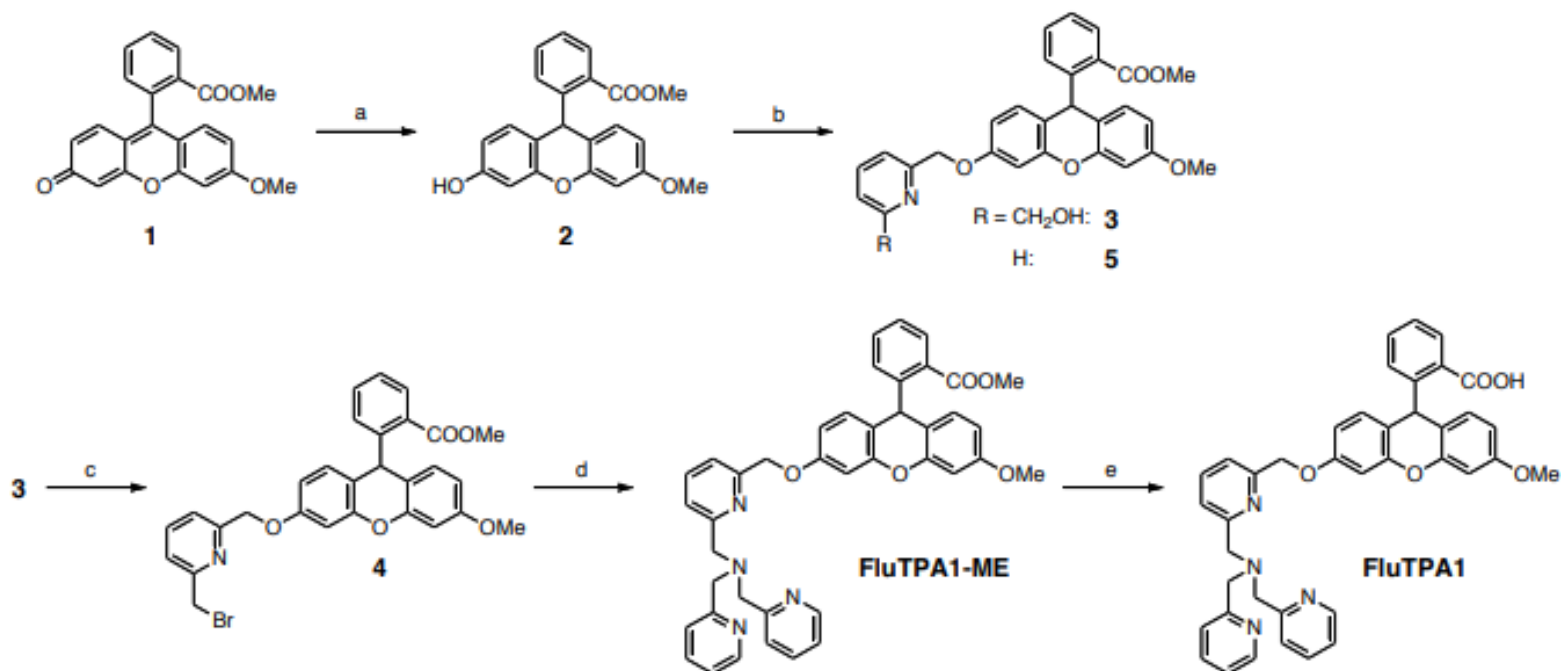


Fig. 1. Synthesis of Coppersensor 790 (CS790) and Coppersensor 790 Acetoxymethyl Ester (CS790AM).



(a) NaBH₄/MeOH, 99 % (b) for **3**: 6-bromomethyl-2-pyridinemethanol, K₂CO₃/MeCN, 94 %; for **5**: 2-(chloromethyl)pyridine hydrochloride, K₂CO₃/MeCN, 72 % (c) PBr₃/CHCl₃, 98 % (d) di(2-picolyl)amine, KI, K₂CO₃/CH₃CN, 93 % (e) NaOH/MeOH-H₂O, for FluTPA1 76 %

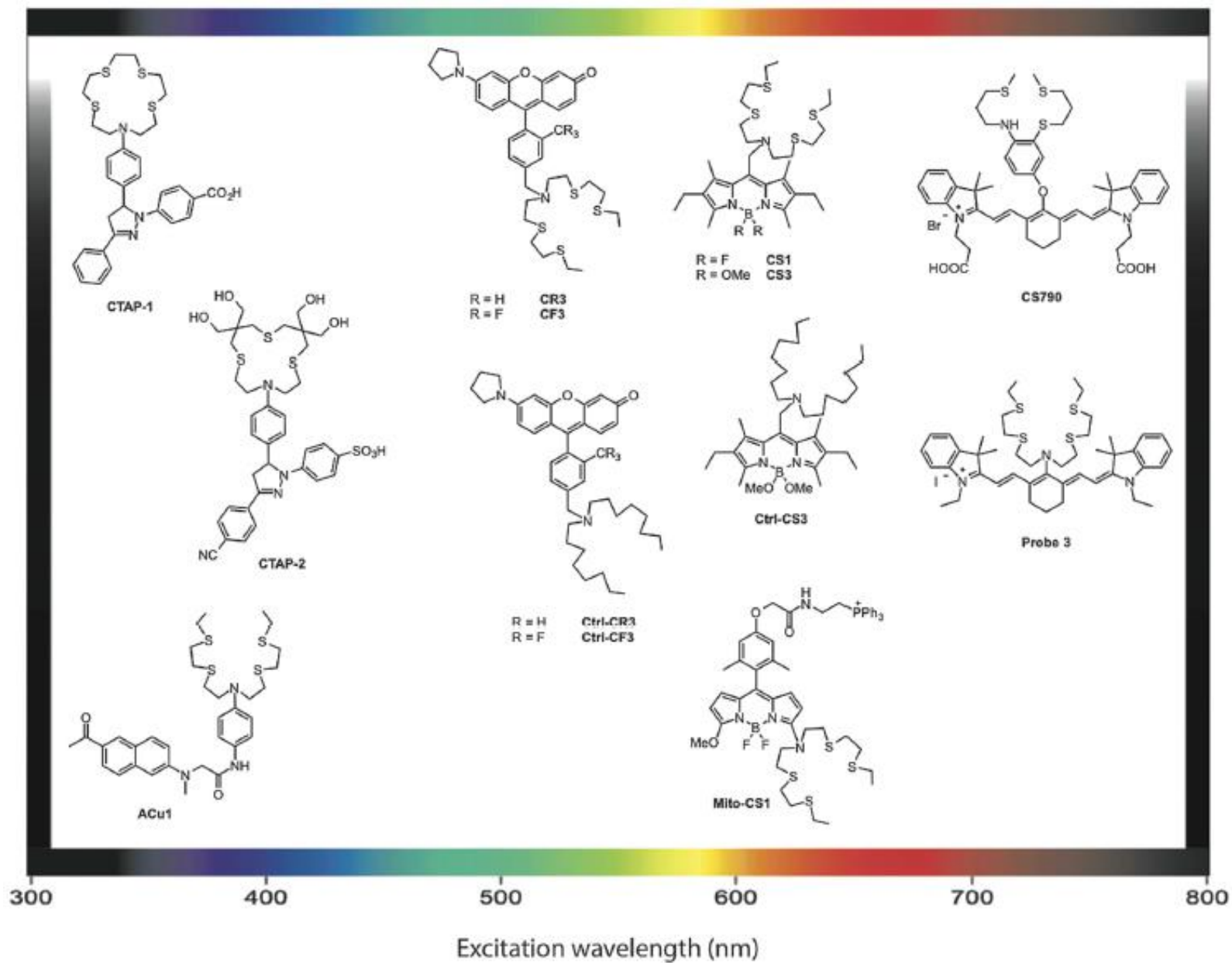
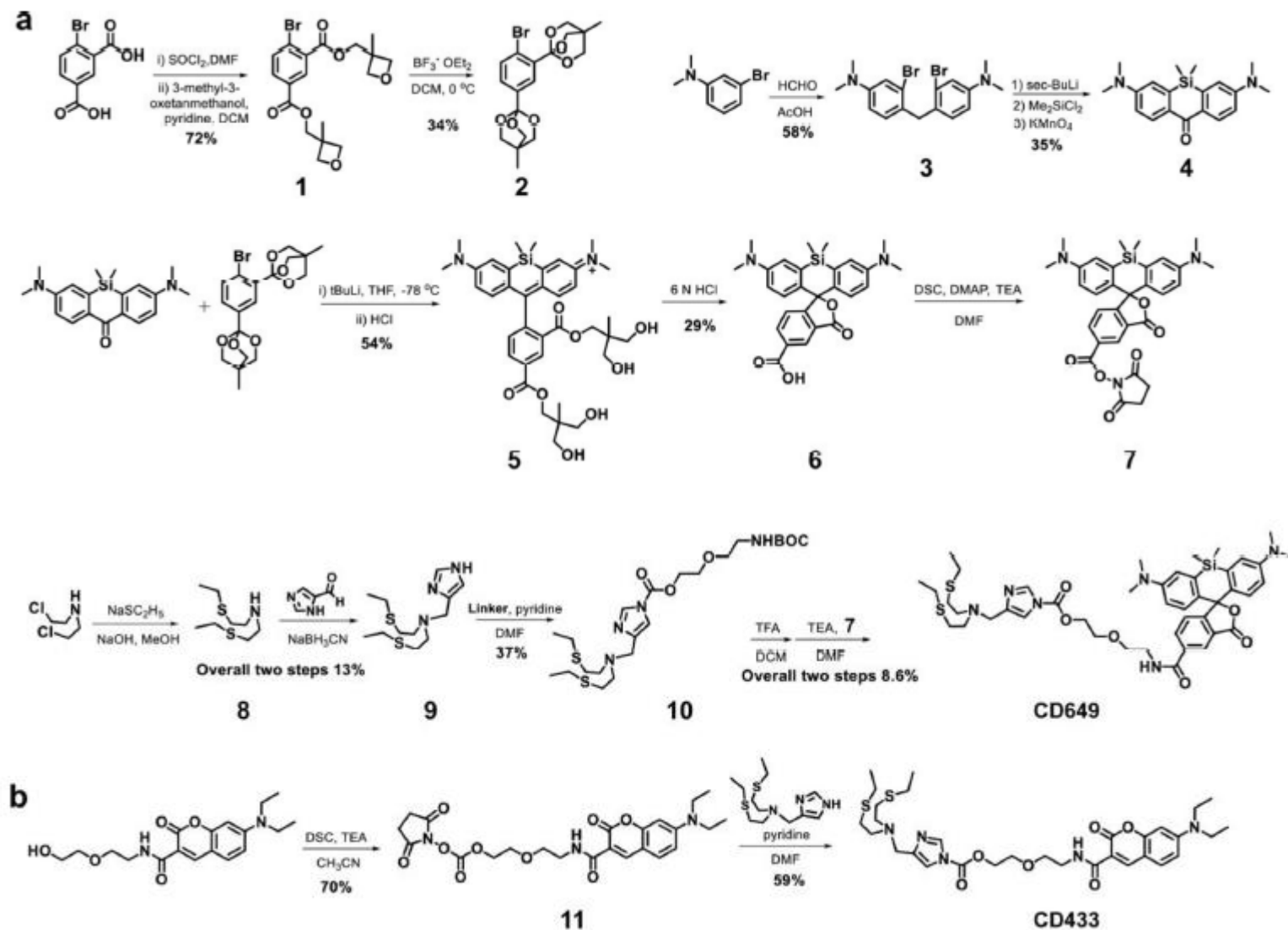


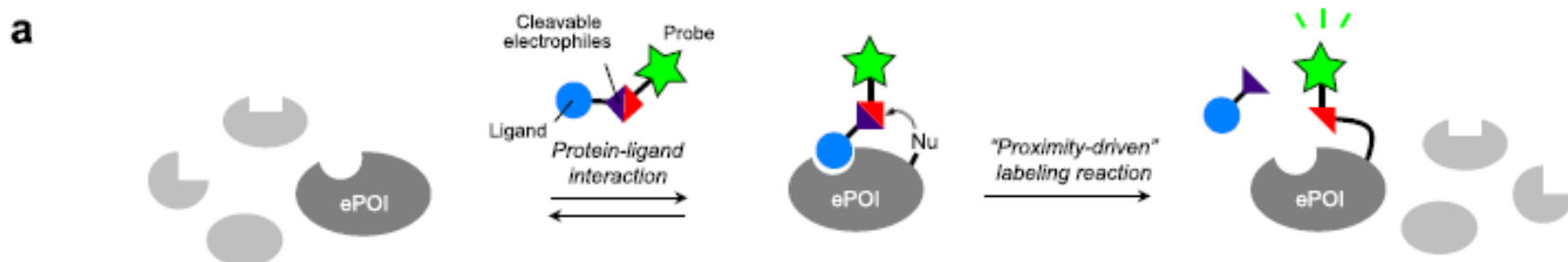
Table 2 Photophysical and thermodynamic properties of selected fluorescent probes for Cu(I)

Sensor	Absorption λ_{max} (nm)	Emission λ_{max} (nm)	Φ^a	f_e^b	K_d (M)	Ref.
CTAP-1	365	485	0.14	4.6	4×10^{-11}	44
CTAP-2	396	508	0.083	65	4×10^{-12}	110
CS1	540	561	0.13	10	4×10^{-12}	111
CS3	540	548	0.40	75	9×10^{-14}	41
Mito-CS1	550	558	0.05	10	7×10^{-12}	112
ACu1	365 (750) ^c	482	0.13 (67) ^c	4	2×10^{-11}	113
CS790	760	790	0.072	15	3×10^{-11}	114
Probe 3	750	792	n.d. ^d	9.6	6×10^{-12}	115
FluTPA1	470	513	0.37	1500 ^f	n.d. ^d	116
CR3	529	545	0.15	13	1×10^{-13}	43
CF3	534 (910) ^c	557	0.22	40	3×10^{-13}	43

^a Fluorescence quantum yield. ^b Fluorescence turn-on *in vitro* [maximum ratio of fluorescence intensity upon Cu(I) binding to intensity of apo sensor]. ^c Value in parenthesis is for two photon absorption. ^d n.d., not determined. ^e Value in parenthesis is two photon absorption cross section ($\Phi\beta$) in GM, at indicated two photon absorption. ^f After 2 h incubation under reported conditions.

Scheme 1. Synthesis of (a) CD649 and (b) CD433; (c) Schematic Cartoon Showing the Working Principle of CD Dyes for Fluorescent Labeling of Proximal Proteins at Sites of Elevated Labile Copper





b

	LDT (2009~)	LDAI (2012~)	LDBB (2015~)	LDSP (2017~)	LDNASA (2018~)
Reactive group	 Tosylate	 Acyl imidazole	 Dibromophenyl benzoate	 N-sulfonyl pyridone	 N-acyl-N-alkyl sulfonamide
k_2 ($M^{-1}s^{-1}$)*	$\sim 10^1$	$\sim 10^1$	$\sim 10^2$	N.D (10 min ~ 6 h)	$\sim 10^4$
Labeled amino acid	His, Tyr, Glu, Asp, Cys	Lys, Ser, Thr, Tyr	Lys, His	Tyr, Lys	Lys
Labeling condition	test tube, inside cells Mucus tissue, lysates <i>in vivo</i> (mouse), etc.	test tube, cell surface, mouse brain tissue (membrane proteins)	test tube, cell surface, inside cells	test tube, cell surface, inside cells	test tube, cell surface, inside cells
Application	^{19}F -NMR biosensor, Fluorescent biosensor, FRET analysis, Photo-cross-link, Ligand-binding site identification	Fluorescent biosensor, Live cell imaging of membrane proteins, Pulse chase analysis, Photo-controlling of enzyme activity, Drug screening	Live cell imaging of intracellular proteins	FRET-based biosensor construction in cells	Covalent inhibition of HSP90